CHEMICAL REVIEWS

REVIEW

pubs.acs.org/CR

Metal−Organic Framework Thin Films: From Fundamentals to Applications.

Angélique Bétard and Roland A. Fischer*

Anorganische Chemie II, Organometallics and Materials, Ruhr-Universität Bochum, D-44780 Bochum, Germany

CONTENTS

1. INTRODUCTION

The field of metal−organic frameworks (MOFs), which are often also called porous coordination polymers (PCPs), has been growing tremendously over the last 15 years. This field has been particularly advanced by Yaghi and co-workers, who coined the acronym "MOF" in 1999 and chose the "yellow sphere" in their artwork to conceptually visualize the volume of free pore in their structure.[1] This fascinating class of crystalline hybrid materials, which are formed by association of metal centers or clusters and organic linker(s), offers a unique chemical versatility combined with a designable framework and an unprecedentedly large and permanent inner porosity. As such, MOFs constitute their own family of porous materials that exceed the limitations of previously known porous materials (zeolites, mesoporous silica, activated carbon).[2]

At first, most efforts were directed toward the synthesis of new frameworks that featured new topologies and open structures with the largest possible surface areas. The goal was to find materials with exceptionally high gas storage capacities, especially for storing hydrogen. More recently, responsive frameworks (in the sense that structures and properties can be controlled by an external parameter (e.g., a guest molecule or physical stimulus)) have been synthesized. Metal−organic frameworks have raised researchers' hopes because of their versatility and extended chemical functionalization relative to zeolites. During the past few years, some of these hopes have started to come to fruition around the concepts of isoreticular frameworks,[3] postsynthesis functionalization,[4] protection/deprotection,[5] solid−solution or multivariate structures (copolymer),[6] and hybrid crystal heterostructure approaches.[7,8] It is now possible to tune the organic linker as well as incorporate reactive groups within a MOF. In addition, the possibility of intentionally creating defects, opening metal sites, and engineering crystal surfaces and internal interfaces has emerged. While efforts continue on the synthesis side, screenings for industrial applications and MOF material processing are also increasingly developing fields. In particular, the processing of MOFs as films is a domain that has only recently been initiated but which is important for many applications, such as chemical sensors[9] and membranes.[10] Inspiration for the

Special Issue: 2012 Metal-Organic Frameworks

Received: May 12, 2011
Published: September 20, 2011

Table 1. Collection of MOFs Films[a]

MOF formula	substrate	method	characteristics, size or thickness	application	ref
$[Cu_3(btc)_2]$ (HKUST-1)	alumina, silica wafers	mother solution at 120 °C	~ 1 μm		18
	α-alumina	seeded growth	~10 μm		19
	SAM on gold	mother solution at 25 °C	preferred orientation, ~600 nm	sensing	20,21
	copper mesh	mother solution at 120 °C	~60 μm	gas separation	22
	copper electrodes	electrochemically	2−20 μm	sensing	23
	copper foil	galvanic displacement	crystallites 100−200 nm		24
	SAM on gold	liquid phase expitaxy	highly oriented, 30−60 nm	mechanistic studies, diffusion coefficient	25−27
	microcantilever	stepwise deposition	~100 nm	sensing	28
	Ag nanoparticles	stepwise deposition		sensing	29
	SAM on gold	gel layer	highly oriented		30
	α-alumina	seeded growth	~25 μm	gas separation	31
	pulp fibers	mother solution at 85 °C			32
	glass slides	deposition of crystals	highly oriented crystals, ~1 μm		33
	SAMs on gold	deposition of crystals	highly oriented crystals, 0.5−1.5 μm		34
	copper slice	mother solution at 25 °C	~5 μm		35
	copper slice	mother solution at 120 °C	~1 μm	humidity sensor	36
	textile (polyester)	stepwise dosing of reactants	~100 nm		37
	porous alumina	seeded growth	~25 μm	gas separation	38
	polymer, oxide, polymer−oxide beads	mother solution at 120 or 25 °C	crystallites ~1−5 μm or ~150 nm		39
	porous polymer monoliths	mother solution at 130 °C	crystallites 0.2−10 μm		40
	SAMs on gold	mother solution (precipitating solvent)	highly oriented ~90 nm		41
$[Zn_4O(bdc)]$ (MOF-5)	oxides wafers, SAM on gold	mother solution at 25 °C	~500 nm		42,43
	graphite/AAO	mother solution in MW	preferred orientation, ~5 μm		44
	graphite/AAO	seeded growth	preferred orientation, ~30 μm	gas separation	45
	α-alumina	mother solution (solvothermal)	25 or 85 μm	gas separation	46
	chromatography column	stepwise deposition	~1 μm	separation	47
	alumina wafer photoresist on silicon	seeded growth	crystallites 20−100 μm		48
ZIF-8	silica wafers	dip coating in mother solution	1−5 μm	sensing	49
	silica wafers	dip coating from colloidal solution	40−500 nm	sensing	50
	porous titania	mother solution in MW	20−30 nm	gas separation	51,52
	α-alumina	seeded growth	preferred orientation, 5−12 μm	gas separation	53
	tubular α-alumina	seeded growth	~5 or 9 μm	gas separation	54

dx.doi.org/10.1021/cr200167v |*Chem. Rev.* 2012, 112, 1055–1083

Table 1. Continued

MOF formula	substrate	method	characteristics, size or thickness	application	ref
	α-alumina	mother solution at 120 °C	~20 μm	gas separation	55
	flexible nylon membrane	slow diffusion (contra diffusion)	~16 μm	gas separation	56
ZIF-7	porous alumina	seeding, then mother solution in MW	preferred orientation ~1.5 μm	gas separation	57−59
	α-alumina	mother solution at 120 °C	~1 μm	gas separation	55
ZIF-22	porous titania	mother solution at 150 °C	~40 μm	gas separation	60
ZIF-69	α-alumina	mother solution (solvothermal)	preferred orientation, ~50 μm	gas separation	61
ZIF-90	α-alumina	mother solution at 100 °C	~20 μm	gas separation	62,63
$[Cu_2(pzdc)_2(pyz)]$	silica wafers	dip coating in mother solution	preferred orientation, ~3 μm		64
SIM-1	α- and γ-alumina beads	mother solution at 85 °C	~15 μm (α-Al_2O_3 only)	heterogeneous catalysis	65
	tubular α-alumina	mother solution at 85 °C	~25 μm	gas separation	66
NAFS-1	silicon wafers	Langmuir−Blodgett technique	highly oriented, 21 nm		67
NAFS-2	gold, silicon	Langmuir−Blodgett technique	highly oriented, ~40 nm		68
$[Zn(bdc)(4,4'\text{-bipy})_{0.5}]$ (MOF-508)	SAM on gold	liquid phase expitaxy	highly oriented, ~40 nm		69
$[Cu_2(ndc)_2(dabco)]$	oxides wafers	stepwise dosing of reactants	preferred orientation, ~120 nm		70
	porous alumina	stepwise dosing of reactants	~30 μm	gas separation	71
$[M(L)(dabco)_{0,5}]$, M = Cu, Zn; L = ndc, F_4bdc	SAM on gold	liquid phase expitaxy	highly oriented, 20−50 nm		72−74
CPO-27-M, M = Ni, Co, Mg, Mn, Zn	alumina wafers	mother solution at 110 °C	2−20 μm		75
MIL-47	polyacrylonitrile	mother solution in MW	several micrometers		76
IRMOF-3/MOF-5	glass slides	mother solution at 105 °C	~10 μm		77
	porous alumina	mother solution at 105 °C	~10 μm	separation	77,78
$[Mn(HCOO)_2]$	α-alumina, graphite	mother solution at 115 °C	preferred orientation, ~300 μm		79
[Al(bdc)] MIL-53	porous alumina	seeding, then mother solution at 220 °C	~8 μm	liquids separation (pevaporation)	80
MIL-96	porous alumina	seeded growth	~10 μm	liquids separation (pevaporation)	80
$[Al_4(OH)_2(OCH_3)_4(H_2N\text{-bdc})_3]\cdot xH_2O$ (CAU-1)	SAM on gold	mother solution at 25 °C	highly oriented, ~150 nm	sensing	81
$[Zn_2(bdc)_2(dabco)]$	oxide wafers	mother solution at 120 °C	~1 μm		18
[Cu(hfipbb) $(H_2hfipbb)_{0,5}$]	porous alumina	seeded growth	preferred orientation, ~20 μm	gas separation	82
In(OH)(bdc)	silicon wafer stainless steel plate aluminum slice α-alumina	seeded growth	~5 μm		83

dx.doi.org/10.1021/cr200167v |*Chem. Rev.* 2012, 112, 1055–1083

Table 1. Continued

MOF formula	substrate	method	characteristics, size or thickness	application	ref
Fe-MIL-88B	SAM on gold	mother solution at 25 °C	highly oriented, ∼500 nm	sensing	84,85
Fe-MIL-88B-NH_2	SAM on gold	slow diffusion (gel layer)	preferred orientation, ∼40 nm		30
MIL-89	silica wafers	dip coating from colloidal solution	40−80 nm	sensing	86
MIL-101(Cr)	silica wafers	dip coating from colloidal solution	20−100 nm	sensing	87
	α-alumina, cordierite monoliths	seeded growth	∼10 μm	heterogeneous catalysis	88
$[Zn_3(btc)_2]$	zinc slide	mother solution at 140 °C	∼20 μm	sensing	89

[a] bdc = 1,4-benzene dicarboxylate; ndc = 1,4-naphthalene dicarboxylate; btc = benzene-1,3,5-tricarboxylate; H_2hfipbb = 4,4′-(hexafluoroisopropylidene)-bis(benzoic acid); dabco = 1,4-diazabicyclo(2.2.2)octane; pyz = pyrazine; F_4bdc = tetrafluoro-1,4-benzene dicarboxylate; pzdc = pyrazine-2,3-dicarboxylate; 4,4′-bipy = 4,4′-bipyridine.

fabrication of MOF thin films often comes from two closely related fields: zeolite films, particularly the direct synthesis and seeded-growth methods, and coordination polymer films in the context of Langmuir−Blodgett and layer-by-layer thin-film preparation techniques. These two areas concern well-known materials and thin-film preparation techniques that are now being translated to MOFs and on which reference literature is abundant.[11,12] Consequently, in this review, we will consider only films made of metal−organic frameworks (MOFs). We define MOFs as hybrid organic−inorganic solid materials made of metal centers or clusters linked together by organic moieties. MOFs feature permanent inner porosities, the reversible adsorption/desorption of guest molecules, and an extended 3D framework with a crystalline structure that can be assessed primarily by X-ray diffraction. Thus, coordination polymer-type films consisting of organic−inorganic hybrid materials that are porous but lack long-range order (e.g., films made of Hofmann clathrates) are beyond the scope of this review. Similarly, ordered films of hybrid but essentially nonporous materials will not be reviewed here. Metal cyanide materials, such as Prussian blue analogs, will not be considered here because the possibility of linker functionalization or isoreticular expansion does not exist at all or is quite limited in contrast to typical MOFs, which allow introduction of functional groups at the organic linkers; more information on Prussian blue analogs can be found elsewhere.[13,14] Also, we rule out all 2D and 1D coordination polymer-type thin films without 3D translational order. In addition, films fabricated from powder MOF material and deposited by, for example, dropping or screen-printing approaches are not considered here because such coatings are not regarded not as "thin" films ($\leq$50 μm).

A typical approach to the preparation of a MOF thin film entails first choosing an existing MOF of interest (e.g., by the size of its pores) and finding a method to process it as a film on top of a given substrate. The film-processing method may be more or less specific to the concerned MOF, which results in a large number of methods that lack generic applicability. In addition, the field is immature and rapidly developing, and a substantial number of important contributions have been published during the last 2 years that were not included in our first review on this subject.[15] Also, the two other most recent reviews on MOF thin films[16] and surface chemistry of MOFs[17] have focused on particular aspects of the general topic. (It was pointed out by one referee of this manuscript that ref 16 also discusses the state of the art of the synthesis and applications of MOF thin films up to the year 2010. We would like to make clear that in ref 16 the emphasis is not on thin-film fabrication but rather on discussion of the perspectives of both existing and future applications. In the present review the synthesis methods and thin-film characterization are systematically and comprehensively discussed, along with selected examples of existing applications only.) The aim of this new and updated review is to offer a systematic and comprehensive treatment of MOF thin films and bring some additional clarity to the reader by rationalizing the existing collection of processing methods from various perspectives. Table 1 gathers *all* examples of MOF thin-film work that correspond to the previously mentioned definition and were available to the authors at the date this manuscript was finalized (July 2011). The listing is organized by the chosen MOF, the type of substrate on which the MOF was deposited or grown, the method for thin-film fabrication, and the intended application of the film, if any. Unless otherwise stated in the characteristics column, the films are polycrystalline and randomly oriented. In addition, an indication of the thickness of the film or size of the crystals is provided. The various methods of the crystals' growth or deposition, combined with a description of the two different classes of MOF thin films, will be discussed in section 2.

In this review, MOF thin films will be examined with respect to three main themes. Fabrication methods are important and will be described in the first section. Characterization, which ranges from compositional and structural identification to lateral homogeneity and porosity, is an important issue that will be discussed together with various strategies aimed at improving the quality and applicability of films. Finally, potential applications of MOF films in several fields will be reviewed.

Two classes of MOF films will be distinguished. Polycrystalline films can be seen as an assembly of more or less randomly oriented MOF crystals or particles that rest on a surface. The crystals can be either well intergrown to completely cover the surface or scattered (presence of holes). In some cases, interactions with the surface favor attachment of crystals in one particular direction with respect to the substrate and each other, which gives rise to preferentially oriented films. The thickness

of such films is related to the size of the MOF particles or crystallites and often lies in the micrometer range. The properties of such films, even if sometimes difficult to evaluate, are expected to be similar to the properties of the bulk powder material. Five main synthesis concepts to derive such MOF thin films can be distinguished and will be discussed in detail. A second, special class of MOF thin films is emerging, which we will call SURMOFs. These films consist of ultrathin (in the nanometer range) MOF multilayers that are perfectly oriented (at least in the direction of the growth). They are very smooth, with roughness on the order of a few elementary cells, and are often quasi-epitaxially grown on the substrate so that the thickness of the film and the crystallite domain size are interrelated and (ideally) can be precisely controlled. The ideal SURMOF would be also characterized by large in-plane single-crystal domains.

The properties of SURMOFs may diverge from their thicker, polycrystalline congeners because of the close proximity of the surface and the slight thickness of the films. Characterization of SURMOFs is even more difficult than that of MOFs and will be discussed separately. Indeed, in some cases, the obtained SURMOF structure simply does not exist as bulk MOF powder or as a single-crystalline material but is accessible only as a thin film bound to an appropriate substrate. SURMOFs also offer the possibility to transfer concepts known from (hard) inorganic condensed-matter single-crystal chemistry and physics to (soft) hybrid inorganic−organic materials, which, most importantly, includes fabrication of heterostructures (MOF on MOF, epitaxially grown) and chemical or structural modifications that are specific for the exposed external surface (top layer) of the films.

2. FABRICATION OF MOF FILMS

Synthesis methods for both SURMOFs and polycrystalline MOF films will be discussed in this section. The requirements for the two classes of films are completely different: providing a true control of the thickness of a SURMOF is much more difficult. Many different methods have been developed to achieve polycrystalline films, but we can group them into five categories, which will be discussed here.

2.1. SURMOFs

To the best of our knowledge, two different methods have been developed to attach a controlled number of unit cells of MOF at a surface, thereby leading to a precise monitoring of the thickness: the liquid-phase epitaxy method and the Langmuir−Blodgett method.

2.1.1. Liquid-Phase Epitaxy. Liquid-phase epitaxy (LPE) relies on the stepwise, layer-by-layer adsorption of components from the liquid phase to a surface. LPE was originally designed for polyelectrolytes held together by ionic interactions.[90] The substrate is alternatively immersed in a positively charged polymer solution and then in a negatively charged solution. The method was soon extended to coordination polymers and metal complexes, for example, with the work of Bell et al.[91] on the Hofmann clathrate [Ni(bipy)(Pt(CN$_4$))]. However, the deposition conditions are rather difficult to meet: the temperature was approximately −60 °C, and each deposition step required 6−8 h. The film deposition of the spin-crossover microporous coordination polymer [Fe(pz)(Pt(CN)$_4$)] was similarly performed by Cobo et al.,[92,93] but no evidence for a crystalline structure based on X-ray diffraction (XRD) was provided.

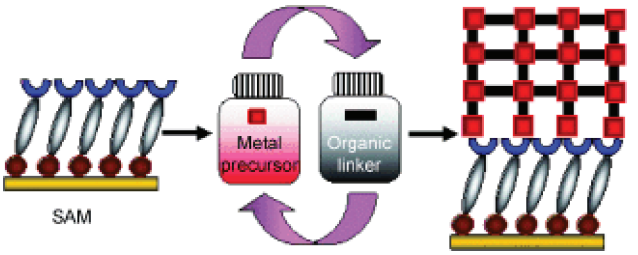

Figure 1. Step-by-step approach for the growth of SURMOFs on a SAM-functionalized substrate. The approach involves repeated cycles of immersion in solutions of the metal precursor and solutions of an organic ligand. Between steps, the material is rinsed with solvent. Reprinted with permission from ref 26. Copyright 2009 Wiley-VCH.

Fischer, Wöll, and co-workers[25] demonstrated in 2007 that the LPE method can also be used to grow MOF films on a surface. The first example was the growth of HKUST-1 ([Cu$_3$(btc)$_2$]). Deposition was performed on functionalized substrates (ideally, self-assembled monolayers (SAMs) on gold) at room temperature or at a maximum 40 °C, and each deposition cycle required 0.5−1.5 h. SAMs were used because of their long-range 2D order, various accessible functionalities, and easy patterning by microcontact printing methods. The organic (e.g., H$_3$btc) and inorganic precursors (e.g., Cu(OAC)$_2$) were placed in ethanolic solutions in separate beakers, and the substrate was sequentially immersed in the two solutions (see Figure 1). Intermediary washing steps with solvent were performed to remove excess adsorbed material. Deposition can be carried out manually or automatically in the cell of certain instruments suited for in-situ monitoring of the growth process, such as surface plasmon resonance (SPR) or quartz crystal microbalance (QCM) measurements. Injection systems on these instruments ensure a continuous flow over the substrate and high reproducibility; meanwhile, each adsorption and desorption (washing) step can be directly observed. Under optimized conditions, the results show a linear growth mode and the number of cycles (and of deposited unit cells) corresponds to the final thickness of the film perpendicular to the substrate surface.[94] The obtained films can be crystalline and highly oriented; the final orientation is mostly controlled by the underlying SAM, which demonstrates the importance of its functionality.[26] In the case of HKUST-1, the film exhibits [100] orientation when the SAM is terminated by COOH groups and [111] orientation when the SAM ends with OH groups. Most remarkably, the choice of the metal component for the growth of HKUST-1 SURMOF by LPE was crucial. When copper(II) nitrate was used as the metal precursor, almost no growth was observed irrespective of the orientation. However, if dimeric copper(II) acetate was employed, the molecular paddle-wheel-type structure which is similar to the metal nodes of the HKUST-1, the growth occurred smoothly. This observation points to the relevance of the so-called "controlled SBU (secondary building unit) approach" (CSA) for SURMOFs.[26,95]

Besides the two-component HKUST-1, three-component [M$_2$(L)$_2$(P)]-type MOF structures (M = Cu, Zn; L = ndc, bdc, or derivatives; P = dabco or 4,4′-bipy) have also been deposited by LPE. Similar to the case of HKUST-1, the metal unit is a paddle-wheel binuclear complex but two different linkers instead of one are present. The dicarboxylic linker L binds to

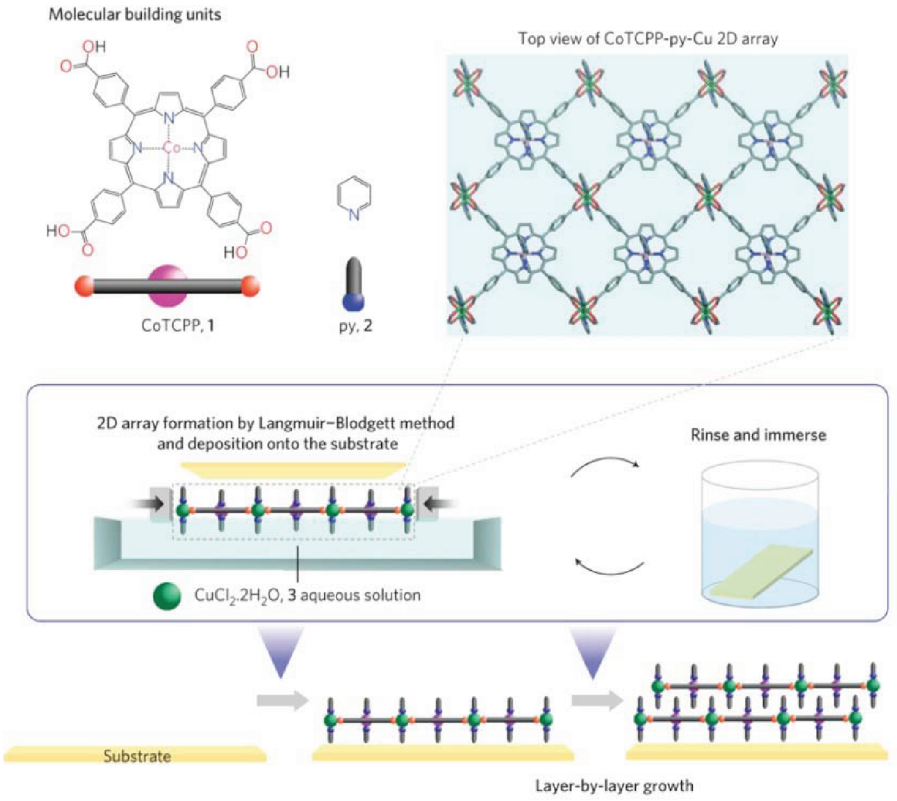

Figure 2. Schematic illustration of the fabrication method of NAFS-1. The solution mixture of CoTCPP (1) and pyridine (2) molecular building units is spread onto an aqueous solution of $CuCl_2 \cdot 2H_2O$ (3) in a Langmuir trough. Pressing the surface with barrier walls leads to formation of a copper-mediated CoTCPP 2D array (CoTCPP–py–Cu) (Langmuir–Blodgett method). The 2D arrays are deposited onto the substrate by the horizontal dipping method at room temperature. The substrate is then immersed in the pure solvent to remove excess starting materials or physisorbed components and subsequently dried. The repetitive process of successive sheet deposition and rinsing/solvent immersion leads to the sequential layer-by-layer growth of NAFS-1 with any desired thickness. Reprinted with permission from ref 67. Copyright 2010 Macmillan Publishers Ltd.: Nature Materials.

the metal complexes to form 2D sheets that are pillared together by the nitrogen-containing linker P. Highly crystalline and smooth SURMOFs are also obtained with this MOF type when CSA is used.[72] Surprisingly, both the underlying SAM and the deposition procedure influence the final orientation. When pyridine-terminated SAMs are used, the two linkers can be mixed, and this solution can be used for growth in a two-step deposition (metal → mixture of ligands) to yield [001]-oriented films. When COOH-terminated SAMs are used, a three-step deposition procedure (metal → dicarboxylic linker → pillar) is necessary to obtain [100]-oriented SURMOFs. This observation may be related to currently unknown effects at the early growth cycles.

2.1.2. Langmuir–Blodgett Layer-by-Layer Deposition. The second method has been developed by H. Kitagawa, R. Makiura, and co-workers.[67] It relies on MOF layers made in a Langmuir–Blodgett (LB) apparatus that are transferred one after another onto a silicon substrate with intermediate rinsing steps. The layers stack by weak interactions, such as π stacking between pendant groups in a manner similar to interdigitated MOFs.[96] The particular MOFs, called NAFS-1[67] and NAFS-2,[68] were achieved using this method; fabrication of NAFS-1 is illustrated in Figure 2. NAFS-1 is made of cobalt-containing porphyrine units (CoTCCP) linked together by binuclear copper paddle-wheel units to form a 2D array. Pyridine molecules bind the axial position of the copper ions perpendicularly to the 2D layers and ensure correct π stacking. The individual sheets are remarkably ordered, with an average tilt angle of 0.3° parallel to the substrate, and the overall thickness of the film corresponds to deposition of one single layer at each cycle. NAFS-2 exhibits a similar structure, the main difference being the absence of the pyridine ligand in the axial position and the porphyrine cage being empty. As a result, the stacking is less efficient with an average tilt angle of 3° between the layers.

The two previously described methods demonstrate proof of principle that it is possible to fabricate ultrathin MOF films, or SURMOFs, in a controlled manner. Such films are interesting both on a fundamental level and on the applications level. However, it is demanding to characterize these films from several points of view: structure identification, porosity, thickness, and lateral homogeneity. A detailed discussion of these issues is presented in section 3.2. It should be noted, however, that the presented examples of SURMOFs fabrication are the only ones known to date. The use of thiol-based SAMs (on gold substrates) for LPE and the water/ambient air interface in the case of the LB technique limits the choices of MOFs in SURMOF growth. Fast kinetics and favorable coordination equilibria are required in these cases. In contrast, many interesting bulk MOFs are synthesized under harsh solvothermal conditions using special solvents, templates, and reactant concentrations, along with pH adjustments and temperatures up to 200 °C. These conditions are not applicable in standard LPE or LB techniques. Thus, for many MOFs, it is seemingly impossible to derive their respective SURMOFs.

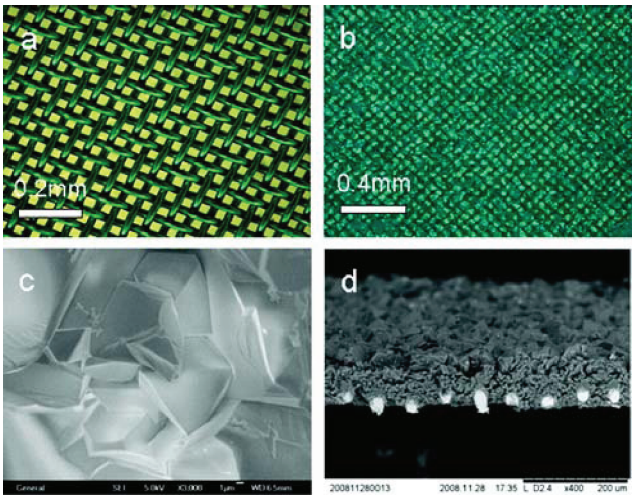

Figure 3. Optic micrographs of the (a) copper net and (b) net-supported $Cu_3(BTC)_2$ membrane; SEM images of (c) the surface and (d) a cross section of the membrane. Reprinted with permission from ref 22. Copyright 2009 American Chemical Society.

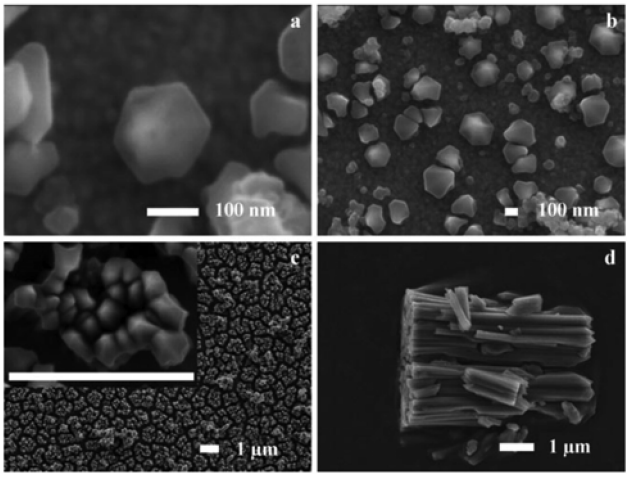

Figure 4. Scanning electron micrographs of Fe-MIL88B crystals sitting on substrates after immersion times of (a,b) 24 h and (c) 3 days. (d) Bundle of removed crystals after 9 days. Reprinted with permission from ref 85. Copyright 2008 Wiley-VCH.

2.2. Polycrystalline Films

2.2.1. Direct Synthesis. Under the name "direct synthesis," we grouped the methods where a substrate is used bare (or modified by organic molecules, i.e., SAMs) together with an appropriate growth solution. Growth takes place at the surface and sometimes also in solution at the same time. This growth leads to formation of crystals attached to the substrate surface in a more or less intergrown and continuous fashion.

2.2.1.1. In-Situ Crystallization. The most straightforward method of preparing a MOF thin film is to prepare a mother solution for a given MOF following the published recipe, insert into the solution one or several substrate(s) (lying face down or vertical is better to avoid sedimentation), and then heating the whole as required for the usual solvothermal synthesis. Despite its apparent simplicity, this method can be quite powerful, especially for oxide wafers,[18,75,77] metal slices,[22,36,89] textiles or fibers,[32,76] and even porous alumina[65,66,79] in some cases. Dense, crystalline, and homogeneous films of micrometer thickness have been obtained by this method.

Zacher et al.[18] studied the morphology of MOF films as a function of the substrate used and showed that the nature of the surface, and especially its acid/base properties, influences whether or not a film can grow. The authors suggested that binding between the surface and the film is mediated by the organic linker, and therefore, an acid-containing MOF (HKUST-1) cannot grow on an acidic surface such as silica. However, a MOF that contains both acidic and basic linkers such as $[Zn_2(bdc)_2(dabco)]$ can grow on both silica and alumina. Arnold et al.[79] reached similar conclusions by studying $[Mn(HCOO)_2]$ on alumina and graphite.

Because the linker seems to play a key role, modification of the substrate with an organic molecule has been proposed to increase heterogeneous nucleation and growth. McCarty et al.[55] modified porous alumina substrates with organic linkers. These researchers dropped linker solutions onto the substrates heated at 200 °C and showed by X-ray photoelectron spectroscopy (XPS) that some linker molecules were covalently bound to Al^{3+} ions. The modified substrates were subsequently inserted into the corresponding ZIF mother solutions and solvothermally treated to yield continuous, well-intergrown films. Huang et al.[60] treated a porous titania support with 3-aminopropyltriethoxysilane (APTES). This molecule is able to bind to the surface by the silane group and thought to act as a covalent linker for binding of ZIF-22 crystals. As a result, the thick (40 μm) and well-intergrown membrane obtained using this linker was of much higher quality than the one obtained without the linker. The same phenomenon has been observed for ZIF-90.[62] In this case, the amino end groups of APTES are thought to react with the aldehyde groups of the linker.

A particularly favorable case is encountered when the substrate is made of the same metal as the MOF to be grown. The substrate's surface is slightly oxidized during synthesis (addition of an oxidant in the reactive mixture may help[35]), which provides metal cations at or near the surface. This phenomenon that favors the anchoring of crystallites is called "twin metal source"[22] and has been demonstrated in the case of copper- and zinc-based MOFs. A good example is the study by Guo et al., who used a copper net as the substrate.[22] The copper net (400 mesh) was first oxidized at 100 °C; the color changed from yellow to green, which indicated the presence of copper oxide. The modified copper net was placed in an autoclave filled with HKUST-1 mother solution and stored at 120 °C for 3 days. A defect-free, homogeneous film with a thickness of approximately 60 μm was obtained (see Figure 3).

Most MOF syntheses take place in conventional ovens. However, microwave-heating approaches have recently been developed for bulk materials and are now being extended to films.[97] The main advantage of this method over conventional heating is the enhancement of the homogeneous reaction and an increased nucleation rate. Indeed, a few hours is typically sufficient to achieve full crystallization. As relevant examples of MOF films, Bux et al.[51] used this method to prepare the first membrane that exhibits molecular-sieving properties (a 40 μm thick ZIF-8 film on a porous titania support), and Centrone et al.[76] described functionalization of polyacrilonitrile by MIL-47 as a function of irradiation time. Yoo et al.[44] introduced a slightly different concept: microwave-induced thermal deposition. The substrates (typically porous alumina) were coated with a conducting layer, such as graphite or gold, and immersed

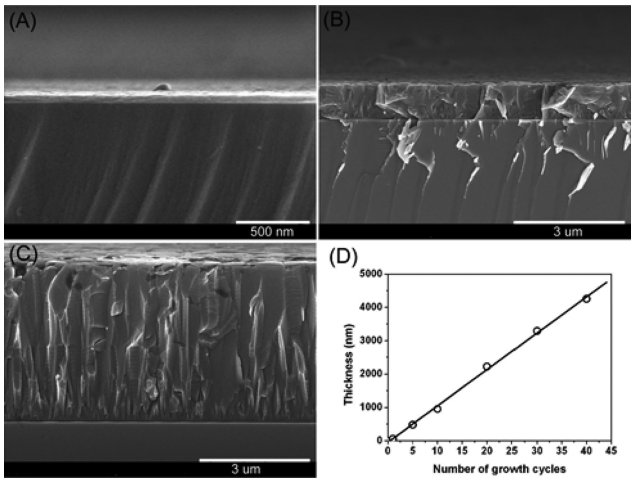

Figure 5. Cross-sectional SEM images of ZIF-8 films grown on silicon substrates with cycles of (A) 1, (B) 10, and (C) 40; (D) thickness of ZIF-8 film versus number of growth cycles. Reprinted with permission from ref 49. Copyright 2010 American Chemical Society.

in a MOF-5 precursor solution. Upon microwave irradiation (5−30 s), the temperature of the conductive layer increased rapidly and induced fast heterogeneous nucleation of MOF-5 crystals. Interestingly, nucleation did not occur in solution but only at or in the immediate vicinity of the surface, which gave rise to a dense MOF layer. The mechanical resistance of the coating was evaluated by 1 h of ultrasonic treatment, where we saw that approximately 80% of the MOF crystals are too strongly bonded to be removed by this method.

2.2.1.2. Growth at Room Temperature. The major problem of the in-situ growth described in the previous section arises from the high temperature used (generally above 100 °C). Indeed, many substrates are temperature sensitive, including self-assembled monolayers (SAMs) on gold, patterned substrates, and integrated devices (e.g., microcantilevers). To address this issue, several groups have separated the nucleation from the crystallite growth. Hermes et al.[42] first introduced this concept in 2005 with MOF-5 as the study case. The authors prepared a mother solution for MOF-5 following published procedures and heated it at 75 °C for 3 days and then briefly at 105 °C to initiate crystallization; they then cooled the solution to 25 °C. The slightly turbid solution was filtrated before being placed into contact with SAM-modified gold substrates. After 24 h, a 5 μm thick film made of MOF-5 crystallites was observed to selectively form on COOH-terminated SAM. The authors suggested that Zn complexes, such as SBU (secondary building units) and/or MOF-5 nuclei, can selectively bind to COOH groups at the surface.

Bein and co-workers extended this approach to several other MOF structures: HKUST-1,[20] Fe-MIL-88B,[85] and CAU-1.[81] They obtained oriented films made of scattered crystals attached in the same direction to the surface. The researchers showed that the functionality of the underlying SAM can direct the orientation of the growth by selectively binding the growth species,[20] and in some cases, the SAM even favors growth of a particular MOF phase.[85] A detailed discussion on control of the orientation is presented in section 3.2.3. The example of Fe-MIL-88B is particularly relevant for demonstrating the importance of the substrate in the fabrications of a film.[85] The authors prepared a Fe-MIL-53 synthesis solution, heated it for 2 days at 150 °C, filtered it, and stored it at 150 °C for 5 days. Afterward, a

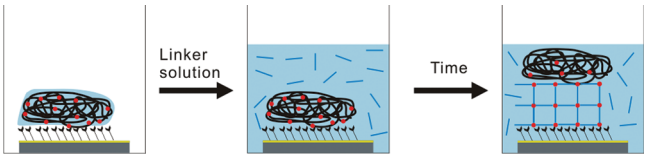

Figure 6. Principle of the gel-layer growth method.

COOH-terminated SAM-functionalized gold slide was immersed in the cold solution for several days. The crystals sitting at the surface were Fe-MIL-88B, whereas Fe-MIL-53 particles formed in solution. The orientation of the crystals on the surface indicated that the 6-fold axis of the MIL-88B crystals was aligned with the apparent hexagonal symmetry of the SAM and that the surface carboxylate groups indeed coordinate to MIL-88B iron atoms. The authors interpreted their results as a symmetry transfer: the SAM exhibits much greater affinity for hexagonal MIL-88B than for monoclinic MIL-53. The morphology of such films is shown in Figure 4 .

The main drawbacks of this method are in the lengthy and sometimes complicated preparation procedure (typically a few days with several heating steps) and the poor morphology of the obtained films. Indeed, the films are often noncontinuous, and the crystals are not really intergrown (Figure 4).

Zhuang et al.[41] recently reported a method for drastically reducing the crystallization time at surfaces. They chose HKUST-1 as case study and prepared a "clear" mother solution in DMSO. A "clear" precursor solution is stable at room temperature, but the MOF is able to crystallize upon evaporation of the solvent.[33] The authors showed that diffusion of vapors of a precipitating solvent (methanol or ethanol) was also able to induce MOF crystallization within a few minutes. Therefore, the precursor solution was applied onto SAM-modified substrates by spin coating, and after exposure to vapors for 20 min, crystals oriented in the [111] direction were found irrespective of the underlying SAM. Interestingly, methanol vapors led to formation of much larger crystals (0.5−1.8 μm) than did ethanol vapors (200−800 nm). This difference was attributed to faster precipitation induced by ethanol compared to methanol. However, because of the small amount of crystals formed on the surface, up to 10 spin coating−exposure to vapors−washing cycles are required to produce dense films. In addition, careful control over the chemistry of MOF nucleation and growth is required.

2.2.1.3. Dip Coating in Mother Solution. In some cases, MOFs crystallize quickly from their mother solution; in fact, they may crystallize as soon as the linker and metal salt are mixed together at room temperature. Kubo et al.[64] took advantage of this fact and grew a film of $[Cu_2(pzdc)_2(pyz)]$ by repeated immersion of a substrate into freshly prepared mother solutions. Bare gold, bare silicon, or SAM-modified gold substrates were all completely covered with densely packed films. The first immersion step allows attachment of some seeds to the surface, whereas the following steps enable both attachment of other seeds and growth of those already present. One immersion step lasted 2 h. Because $[Cu_2(pzdc)_2(pyz)]$ tends to form plate-like crystals and thereby expose the (010) facet, the resulting films show a preferred orientation along the *b* axis. Notably similar results were obtained when ZIF-8 was used instead of $[Cu_2(pzdc)_2(pyz)]$.[49] No preferred orientation was found, but growth was much more regular (about 100 nm per cycle), and a continuous film was formed from the first layer (see Figure 5).

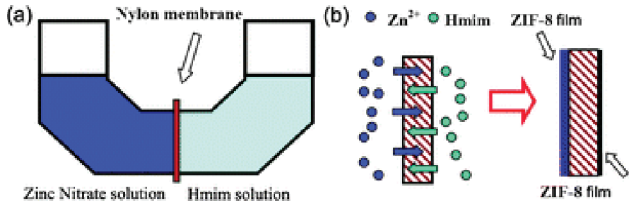

Figure 7. (a) Diffusion cell for ZIF-8 film preparation, and (b) schematic of the formation of ZIF-8 films on both sides of the nylon support via contradiffusion of Zn^{2+} and Hmim through the pores of the nylon support. Reproduced with permission ref 56. Copyright 2011 The Royal Society of Chemistry.

2.2.1.4. Slow Diffusion of Reactants. As a consequence of the fast MOF nucleation rate, crystals are preferentially formed in homogeneous solution rather than at the liquid/solid interface of the substrate. To overcome this drawback, Bein and co-workers[30] introduced a method for MOF thin-film growth that is often used in bulk synthesis to obtain single crystals instead of microcrystalline materials: slow diffusion of reactants in a gel.[98] A poly(ethyleneoxide) (PEO) gel layer was loaded with the MOF metal-ion precursor and deposited onto a SAM-modified gold-coated substrate. The gel layer was then covered with a linker solution, which allowed the linker to slowly diffuse into the gel, and MOF nucleation was successfully directed at the interface provided by the substrate (see Figure 6).

Because of this method, a high local concentration of metal ions is achieved near the surface, which leads to a high heterogeneous nucleation rate of the MOF and therefore to film growth within a few days. Parameters such as the chain length of the PEO and the concentration of metal ions in the gel can be varied to control the morphology and thickness of the final film. In the case of HKUST-1, a perfect orientation along [111] is observed, which is independent of the functionality of the underlying SAM (COOH or OH). These results are different from growth in a mother solution at room temperature (section 2.2.1.2) where COOH and OH SAM functionalities lead to different orientations. In the case of the flexible Fe-MIL-88B_NH_2, a highly oriented film along [001] was obtained only on COOH-SAM.

When the substrate is a (macroporous) membrane, it is also possible to use it as a permeable separator between the metal salt and the linker solutions. Similar to the fabrication mechanism of single crystals by slow diffusion, metal and linker ions are able to cross the membrane and crystallize at the interface (see Figure 7). This principle was recently applied for fabrication of ZIF-8 films on flexible porous nylon membranes.[56] ZIF-8 crystalline layers were observed on both sides of the substrate with the layer at the zinc side being thicker. After 72 h, a continuous film of approximately 18 μm in thickness was formed on the zinc−nitrate side, whereas small scattered nanoparticles were formed on the linker side. Interestingly, the morphology and thickness of the film can be controlled by varying the concentration of the solutions, synthesis time, and number of repetitions. The gas separation permeances of the membranes were also tested. Surprisingly, the best results showed higher permeances but lower H_2/N_2 selectivities (4.3) compared to ZIF-8 membranes made by direct synthesis under solvothermal conditions (11.6).[51] The membrane obtained by slow diffusion may, therefore, be of lower quality.

2.2.1.5. Controlled Deposition of Crystals at a Surface. An original method of preparing MOF crystallites at surfaces was

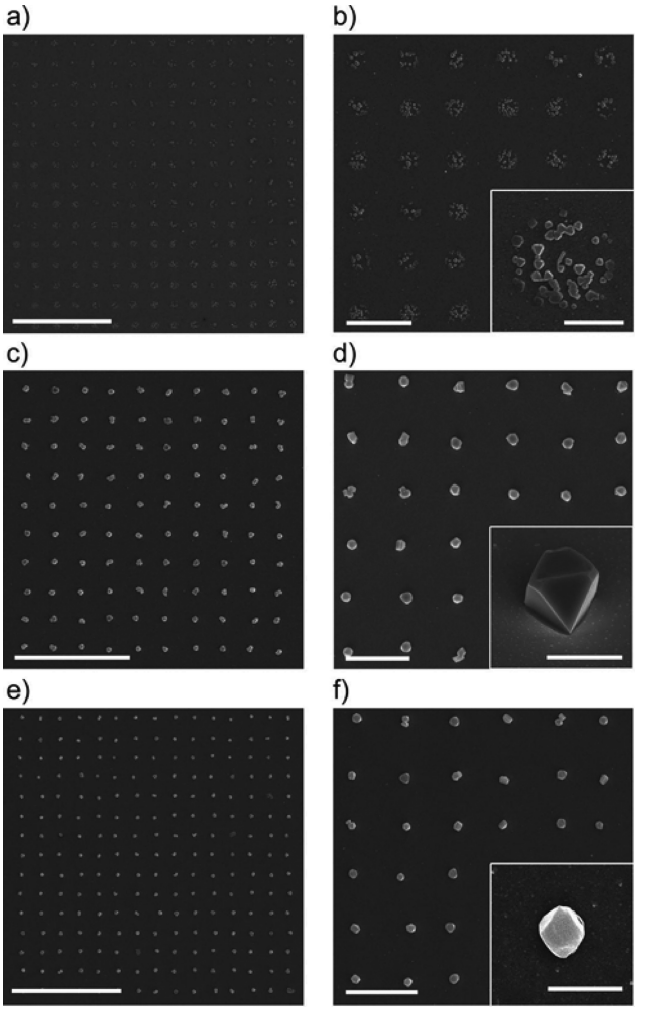

Figure 8. SEM images of the HKUST-1 arrays fabricated on (a, b) NH_2-, (c, d) CH_3-, and (e, f) CF_3-terminated SAMs on gold substrates. Scale bars represent (a, c, e) 40, (b, d, f) 10, and (insets) 2 μm. Reprinted with permission from ref 34. Copyright 2011 American Chemical Society.

proposed by Ameloot et al.[33] This method relies on the mixing of precursors in an appropriate solvent to form "clear solutions", i.e., solutions from which no MOF precipitates at room temperature. However, the MOF is obtained when the solvent is evaporated from those solutions. PDMS stamps were inked with such a solution of HKUST-1 precursors and applied onto a surface. Upon being heated at 100 °C, the solvent slowly evaporates and the MOF crystallizes. The authors observed that the crystallites show a preferred orientation along the [111] axis independent of the nature of the substrate. This result shows that confinement rather than substrate functionalization is able to orient the growth. The typical crystallite size is 1−2 μm.

In a related study, Carbonell et al.[34] produced arrays of HKUST-1 single crystals. In their approach, the substrates were homogeneously covered with various SAMs. Droplets of clear mother solution (3−5 μm large) were subsequently deposited onto the surface by a pen-like surface-patterning tool, which was automatically controlled. The solvent was evaporated under ambient conditions, which led to formation of HKUST-1 crystals. In the case of hydrophilic SAMs (COOH and OH terminated), the droplets spread completely, whereas on

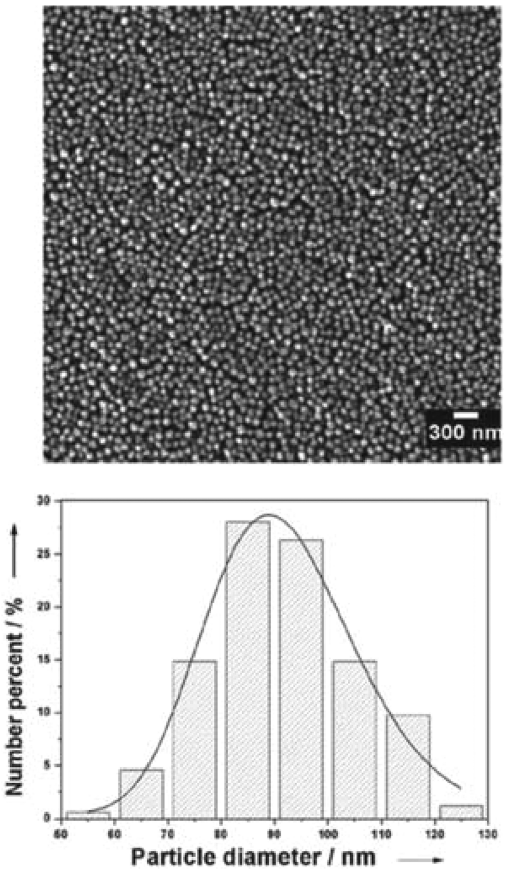

Figure 9. SEM image of ZIF-7 nanoparticles used as seeds in ref 58. Size distributions were determined by image analysis. Reprinted with permission from ref 58. Copyright 2010 Wiley-VCH.

hydrophobic CH_3- and CF_3-terminated SAMs, the droplets were confined and single crystals approximately 1 μm in size formed (see Figure 8). Here again, the crystals were oriented in the [111] direction. Interestingly, the size of the final crystals can be easily controlled by the volume of the droplet, which in turn is controlled by the plasma treatment of the patterning tool.

2.2.2. Seeded Growth. Seeded growth, also called secondary growth, is a common method, particularly in zeolite film fabrication.[11,12] Because the heterogeneous nucleation density of many MOFs is low on porous ceramic supports, the method has become more popular for MOF thin-film fabrication. The method requires two steps: preparation and deposition of seeds followed by growth into a film. Various kinds of seeds may be used and will be described below. The secondary growth step is often performed under solvothermal conditions.

2.2.2.1. MOF Nanocrystals. The most commonly used seeds are nanocrystals (size 20−100 nm) of the desired MOF. After their synthesis and characterization, they are deposited onto the substrate, typically by dropping or spin coating. The availability of such MOF nanocrystals is sometimes a difficult issue, although more synthesis protocols are being published,[99] and such concepts as "coordination modulators"[100] have appeared to help control the size and shape of MOF nanocrystals. Larger crystals, typically in the micrometer range, are not suitable.[19] In a typical seeded growth experiment, such as the one carried out by Zou et al.,[83] colloidal seeds of In(OH)(bdc) were first synthesized and isolated. They were then redispersed in

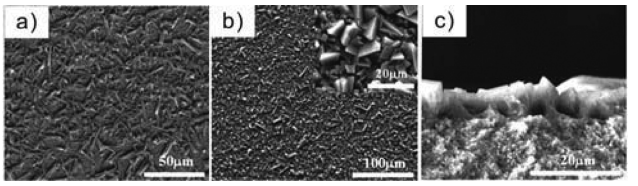

Figure 10. SEM images of (a) MIL-53 seeds, (b) MIL-53 membrane, and (c) a cross section of a MIL-53 membrane. Adapted from ref 80 with permission of The Royal Society of Chemistry.

methanol to produce a white colloidal solution that was dropped onto various substrates, including a silicon wafer and a porous α-alumina disk. After drying, the substrates were placed vertically in autoclaves filled with the mother solution and solvothermally treated for 3 days. The obtained layers were approximately 5 μm thick and made of compact packings of hexagonal-disk-shaped crystals. Sometimes, as in the case for MOF-5, the seeds are not really stable in the solution used for secondary growth and either dissolve or dissociate from the substrate. If dissolution occurs, the acidic properties of the linker are often responsible, and addition of a base, such as *N*-ethyldiisopropylamine, may be necessary to produce a film after the secondary growth step.[45]

A problem often encountered is the lack of adhesion between the seeds and the substrate. Ranjan et al.[82] first deposited a polyethyleneimine (PEI) layer on the surface and manually deposited seeds of $[Cu(hfipbb)(H_2hfipbb)_{0,5}]$ on the PEI layer. An enhanced attachment of seeds via H bonding was expected. After solvothermal treatment, a crack-free layer of approximately 20 μm thick was observed on the surface. In spite of randomly oriented seeds, the final layer shows preferred orientation in the *b* direction, which corresponds to pores that are perpendicular to the substrate. Li et al.[57,58] obtained similar results with ZIF-7. The seeds were synthesized either alone or in the direct presence of PEI and were then transferred onto the substrate by dip coating (see Figure 9 for typical seeds). Addition of diethylamine as a deprotonating agent in the mother solutions during the secondary growth step enabled growth of a preferably oriented film from a randomly oriented seeding layer (see section 3.2.3 for more details).

Again aiming at increasing adhesion between the seeds and the substrate, Varela-Guerrero et al.[31] introduced the concept of "thermal seeding" for HKUST-1 on porous alumina substrates. Their inspiration comes from zeolite films. Indeed, seeds can be deposited on a surface and calcined such that the hydroxyl groups at the substrate's surface react with those of the zeolite. Such an approach is, of course, not possible with HKUST-1 because of the lack of OH surface groups. Nevertheless, the authors demonstrated that dropping the seeds onto a hot substrate (200 °C) rather than a room-temperature substrate favors anchorage of the seeds and leads to formation of dense and homogeneous films after the secondary growth step.

Hu et al.[80] developed an interesting "reactive seeding" approach to growing MIL-53 (Al) on a porous alumina substrate. Similar to the case of metal substrates discussed in section 2.2.1.1, the substrate is used as a metal source for nucleation of the seeds. Film fabrication consists of two steps. First, the substrate is incubated with the linker only under mild solvothermal conditions to produce a seed layer. Next, the modified substrate is immersed into a MIL-53 (Al) mother solution for the secondary growth step at 220 °C. SEM inspections (Figure 10) showed that

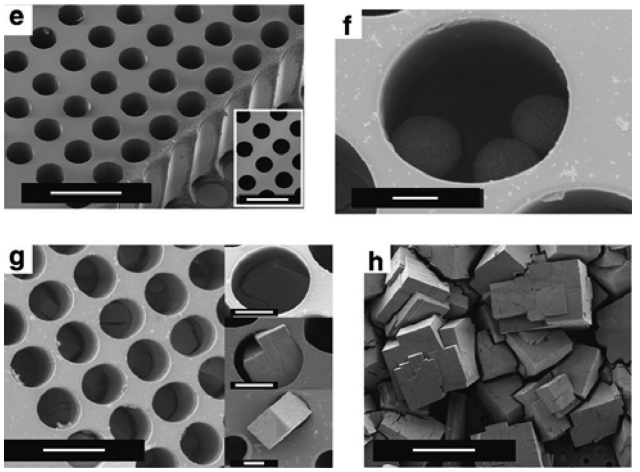

Figure 11. Desert rose microparticles used for positioning MOF-5 on patterned supports. (e) SU-8 membrane obtained after the lithographic procedure. The wells have a diameter of 40 μm and depth of 100 μm (scale bar, 100 μm). (f) DRMs located in a hole of the substrate after the drop-casting and drying processes (scale bar, 10 μm). (g) MOF-5 crystals growing within each of the lithographed holes. The micrograph was taken after 5 h reaction time at 95 °C in the MOF-5 growing medium (scale bar, 50 μm). The insets show crystals emerging from the holes during growth (scale bar, 20 μm). (h) Substrate after 10 h reaction time at 95 °C. MOF-5 crystals have grown out of the holes and appear to be interconnected with their neighbors, which is a prerequisite for controlled formation of a continuous layer of MOF (scale bar, 200 μm). Reprinted with permission from ref 48. Copyright 2011 Nature Publishing Group.

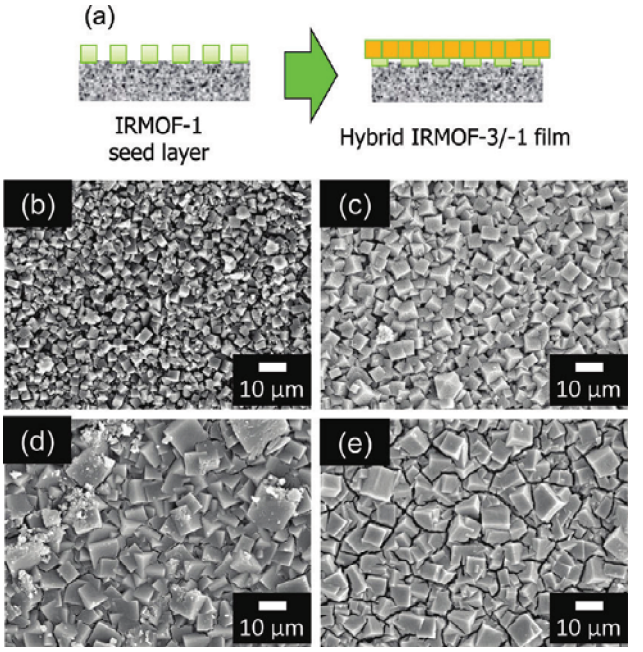

Figure 12. Schematic illustration of heteroepitaxially grown IRMOF-3 on the surface of an IRMOF-1 seed crystal layer (a), and SEM images of an IRMOF-1 seed layer (b). IRMOF-3/-1 hybrid films grown for 1 (c), 2 (d), and 3 h (e). Reprinted with permission from ref 77. Copyright 2010 American Chemical Society.

the seeds were homogeneously distributed at the surface and that a dense, crack-free MOF layer with a thickness of approximately 8 μm was formed.

2.2.2.2. Non-MOF Particles as Seeds. Falcaro et al.[48] developed a novel method for fabrication of seeds for subsequent MOF growth. They prepared a MOF-5 growth solution in DMF in the presence of the commercial surfactant Pluronic F-127. The surfactant both coordinates the zinc ions and provides phosphates in the reaction medium. As a result, polyhydrate zinc phosphate rapidly precipitated in the form of nanoflaked microparticles (called desert rose microparticles or DRMs). After being isolated and inserted into an MOF-5 synthesis solution in DEF at 95 °C, these particles act as heterogeneous nucleation seeds for MOF crystals. High-quality crystals were obtained in a short time. Interestingly, these seeds can be used either dispersed in solution or attached to a surface. Seeds dropped on flat oxide surfaces (alumina, silica) and also on patterned substrates (see Figure 11) induce MOF growth on surfaces in the form of large intergrown crystals.

2.2.2.3. Coordination Polymers as Seeds. Gascon et al.[19] studied the use of various coordination polymers as seeds for MOF coatings on porous alumina substrates. They chose HKUST-1 as a test system and used as seeds micrometer-sized crystals, one-dimensional Cu(II)−BTC coordination polymer, or amorphous HKUST-1 precursors. The seeds were prepared separately, dispersed in solvent, and spin coated onto the substrates. The one-dimensional Cu(II)−BTC coordination polymer was obtained by replacing ethanol with water in a HKUST-1 mother solution to prevent full deprotonation of the BTC linker, which formed well-defined tagliatelle-like structures. The amorphous precursor is made of the powder material that precipitates as soon as the copper nitrate and trimesic acid are mixed in a water/ethanol solution. This material is amorphous and transforms into the MOF structure upon solvothermal treatment. The authors showed that when crystals (5 μm) were used as seeds, few new nucleation events occur during the secondary growth step and big crystals were found scattered at the surface. However, use of the coordination polymer or amorphous precursors led to homogeneous layers of HKUST-1 that were randomly oriented with thicknesses ranging from 2 to 5 μm.

The stepwise deposition of reactants is another method of depositing MOF precursors on surfaces (see section 2.2.5). Nan et al.[38] performed four deposition cycles of HKUST-1; using AFM, they observed formation of copper carboxylate complexes at the surface, which acted as seeds. After a secondary growth step at 120 °C, a 25 μm thick dense MOF layer was obtained.

2.2.2.4. MOF Thin Films as Seed Layers. Recently, several works showed that thin MOF layers can also be used as seeding layers to grow thicker MOF films. Yusenko et al.[70] constructed a $[Cu(ndc)(dabco)_{0,5}]$ film by stepwise dosing of reactants (see section 2.2.5) and used this film as a seeding layer for a secondary growth step. This last step was performed in a typical $[Cu(ndc)(dabco)_{0.5}]$ mother solution under solvothermal conditions for 12 h. Compared to a direct growth method in a mother solution, the film obtained by seeded growth was more homogeneous and continuous and retained the preferred orientation of the seeding layer.

Yoo et al.[77] studied the system MOF-5/IRMOF-3 in detail. They first grew hybridized single crystals with MOF-5 as the core and IRMOF-3 as the shell and then used this knowledge to grow hybrid films. Indeed, no satisfactory films of IRMOF-3 are obtained either from direct synthesis under solvothermal conditions or from microwave-induced thermal deposition because

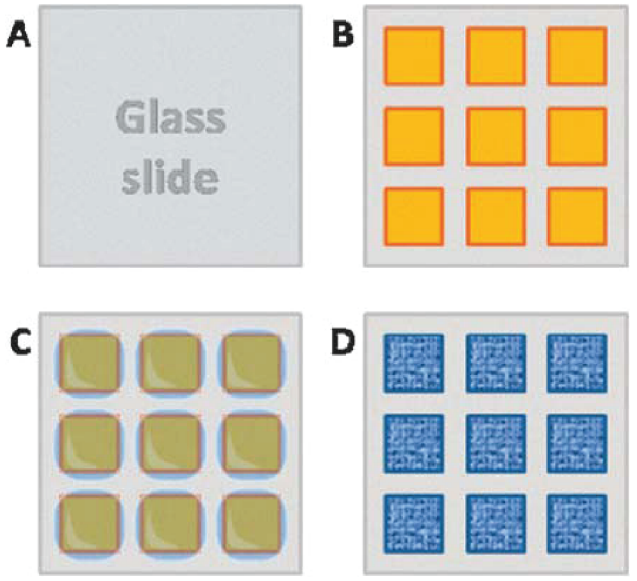

Figure 13. Schematic illustration of patterned film growth of $[Cu_3(BTC)_2]$ by galvanic displacement. A glass slide treated with chlorotrimethylsilane (A) is covered with metallic copper in a patterned way (B). A solution of silver nitrate and H_3BTC in DMSO is subsequently spin coated onto the slide (C). After evaporation of the solvent, the metallic pattern is covered by $[Cu_3(BTC)_2]$ crystallites (D). Reprinted with permission from ref 24. Copyright 2010 The Royal Society of Chemistry.

the heterogeneous nucleation rate of IRMOF-3 is very low. Therefore, the authors decided to grow MOF-5 layers on their substrates first and then performed a secondary growth step in a IRMOF-3 mother solution. Figure 12c−e shows images of the resulting films when porous alumina was used as the substrate (the seeding layer was grown by microwave-induced thermal deposition). When the time allowed for growth was increased from 1 to 3 h (Figure 12c−e), the crystals increased in size and became intergrown. The cracks in the films are due to the instability of IRMOF-3 toward air when dry. Solutions to this problem will be discussed in section 3.2.2.

2.2.3. Electrochemical Methods. Electrochemical methods to synthesize MOFs were first introduced by scientists at BASF for the large-scale production of MOF powders.[101] A metal electrode is oxidized to provide metal ions in a solution that contains the ligand. Ameloot et al.[23] showed that, by modifying the conditions and in the absence of stirring, it is possible to coat the metal electrodes by a MOF film. The case study of the authors involved growth of HKUST-1 on copper anodes. By applying an anodic voltage to copper electrodes immersed in a BTC solution, MOF layers were formed in 30 min or less. Various thicknesses (2−50 μm) and intergrowth degrees could be obtained by variation of the water content of the solution as well as the voltage and frequency of the applied tension. Because the metal ion is supplied at the surface where nucleation takes place, the crystals, and thus the resulting films, are remarkably homogeneous. To the best of our knowledge, only HKUST-1 has been grown using this method. Nevertheless, fabrication of other MOF films featuring other transition metals should be possible.

In a more recent work, the same group[24] reported a new growth method based on galvanic displacement. Here again, metallic copper was used as a source to build HKUST-1 MOF. The fabrication scheme is depicted in Figure 13. A film of metallic copper was first deposited onto a substrate (e.g., a glass slide) by thermal evaporation. A solution of silver nitrate and BTC ligand in DMSO was then spin coated over the copper-coated substrate, and the coated substrate was heated at 80 °C until complete evaporation of the solvent. By reaction of silver ions and copper film, Cu^{2+} ions are produced and silver ions are reduced to metallic silver (galvanic displacement), which provides the necessary building blocks. Homogeneous coatings made of small, intergrown, and octahedral HKUST-1 crystallites (100−200 nm) are formed. Adhesion of the MOF film to the substrate is strong because it cannot be peeled off by sonication. The drawback of this method is that, in spite of extensive washing, metallic silver particles contaminate the resulting film.

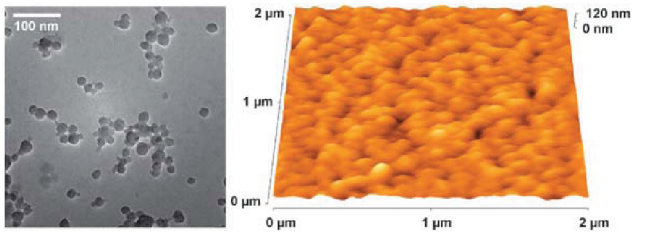

Figure 14. TEM (left) and AFM (right) images of nanoparticles and a 97 nm thin film of MIL-101(Cr), respectively. Reprinted with permission from ref 87. Copyright 2009 The Royal Society of Chemistry.

2.2.4. Assembly of Preformed MOF Nanocrystals. Fabrication of MOF films by assembly of preformed objects (typically colloids) has been extensively studied by Sanchez, Serre, and co-workers.[50,86,87] Their approach is to prepare well-defined MOF particles and transfer them onto a surface by dip coating. To prove the generality of the concept, the authors experimented with three different MOF structures: the iron muconate MIL-89,[86] MIL-101 (Cr),[87] and ZIF-8.[50] The advantages of such a route over other routes are precise control of the particle size and the presence of intergrain mesoporosity. Combined, these two advantages enable easier diffusion of analytes into the film and can be useful for certain applications. In this review, we describe the case of MIL-101 (Cr) as a typical example. The first step is preparation of a stable colloidal and homogeneous dispersion of MIL-101 (Cr) nanocrystals. This step was achieved by a short synthesis (1 min) under microwave irradiation. Nanoparticles with an average diameter of 22 nm were harvested and characterized to confirm their chemical identity. Next, the particles were redispersed in ethanol to form a stable colloidal dispersion into which a bare silicon substrate was dip coated. Depending on the concentrations of particles in solution, 2−3 layers of particles were deposited at a time. Repetition of the dip-coating process led to thicker films and allowed close control of the thickness. The nanoparticles appear to closely pack and form relatively uniform layers (see Figure 14). However, the mechanical resistance of such films, which are not rigidly linked to their substrates, is questionable.

2.2.5. Stepwise Dosing of Reagents. The stepwise dosing of reagents is a deposition method closely related to the liquid-phase epitaxy method described in section 2.1.1 but is more general. Indeed, the method concerns depositions where the conditions required for linear layer-by-layer growth, specifically, a SAM-modified gold substrate and manual or in-situ-automated deposition featuring continuous flowing are not reunited. Nevertheless, the principle of separating reagents and dosing them stepwise onto a surface is kept and applied

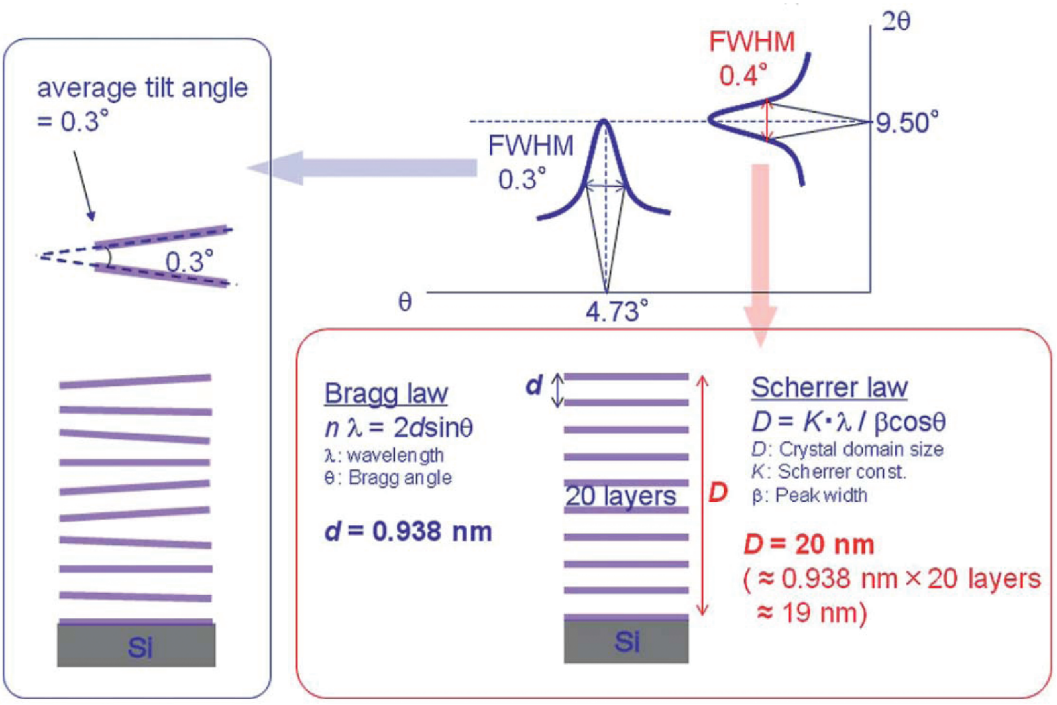

Figure 15. Derivation of the interlayer spacing and film thickness from out-of-plane synchrotron XRD measurements. Reprinted with permission from ref 102. Copyright 2010 Wiley-VCH.

to various substrates, including inorganic wafers,[70] textiles,[37] and porous alumina.[71] Using $[Cu_2(ndc)_2(dabco)]$ as a test system, Yusenko et al. studied inorganic wafers (SiO_2, Al_2O_3, Ta_2O_5, and Si_3N_4) and showed that the growth is not self-terminated but is rather the result of a complex equilibrium between the metal-ion ligands (here acetates) and the organic linkers. A higher temperature (about 50 °C) is also required. Moreover, storage of precursors in the already-grown structure increases their local concentration. As a result, after 40 deposition cycles, the films consisted of 100 nm discrete crystals that were intergrown and formed a rough 120−150 nm thick film instead of the very smooth, 40 nm thick SURMOF film one would expect on a SAM-modified substrate. Interestingly, the films showed preferential orientation in the [001] direction and can be used as a seeding layer for growth of a thicker film (see section 2.2.2.3). The orientation of such films is controlled not merely by the functionality of the substrate but also by the deposition sequence. Indeed, using a three-step deposition instead of a two-step one (as detailed in section 2.1.1) led to [100]-oriented films without any difference in surface preparation.[71]

3. CONTROLLING AND CHARACTERIZING MOF FILMS

3.1. SURMOFs

3.1.1. Characterization. Because of their very small thickness, SURMOFs raise specific characterization issues, including structural characterization, morphology, and porosity measurements. In the following sections, we will describe relevant techniques as well as some examples of their use for the characterization of SURMOFs.

3.1.1.1. Crystalline Structure. The tool usually used for structural assignment of films is X-ray diffraction. Two scattering geometries are relevant: the out-of-plane mode and the in-plane mode. The out-of-plane geometry is a simple Bragg−Brentano geometry and can be performed with simple laboratory equipment, but it is sensitive only to the lattice parameter that is parallel to the substrate (i.e., in the growth direction). The in-plane geometry (at grazing incidence) is sensitive only to in-plane lattice dimensions. Therefore, to obtain the complete XRD pattern for a highly oriented film, both measurements are needed. Due to the thickness of typical SURMOFs (20−50 nm) and the low density of the material, synchrotron radiation might be necessary. In most cases, the MOF structure has been already described as bulk, and a simple comparison between patterns enables assignment of the structure. However, it is also possible to grow films with corresponding structures that cannot be obtained as a single crystal or as a powder.[67,69] In such cases, models should be used together with XRD data. In the case of NAFS-1,[67] a complete structural model was built starting from related known structures and was compared to X-ray data for evaluation. XPS and IR spectroscopy also gave useful information about the degree of oxidation and the coordination states of metal ions and were helpful in building the model.

In addition to structural studies, X-ray diffraction can also provide some insights into the morphology and homogeneity of a given sample. Domain sizes can be calculated using either the Scherrer equation or more advanced tools, such as Fourier single-line analysis. For a SURMOF with a self-terminated, linear growth mode, the domain size in the growth direction corresponds to the number of applied cycles multiplied by the cell dimension.[67,72] Measurement of rocking curves (θ scan) and the sample direction dependence at one specific peak position can also give useful information. In the study by Makiura et al.,[37] the (001) line in the out-of-plane mode was chosen because it reflects the stacking of layers. Rocking-curve measurements gave a single peak with a full width at half-maximum (fwhm) of 0.3°, which indicated that the layers are nearly parallel to each other (average tilt angle of 0.3°) (see Figure 15). The sample direction

dx.doi.org/10.1021/cr200167v |*Chem. Rev.* 2012, 112, 1055–1083

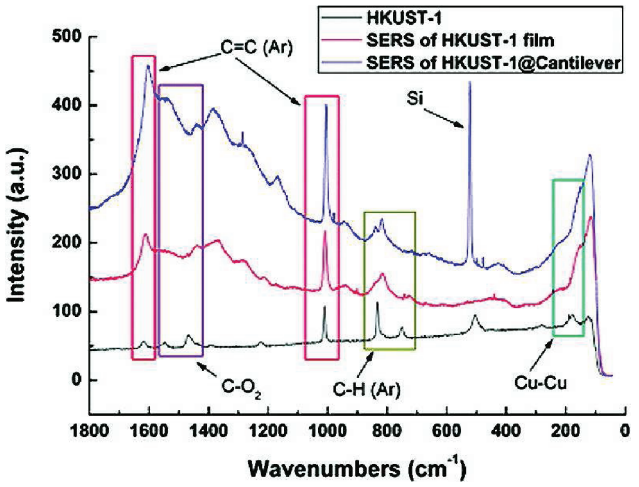

Figure 16. Verification of HKUST-1 on the microcantilever using SERS: (blue) SERS spectrum of HKUST-1 on a microcantilever; (red) SERS spectrum of an HKUST-1 film on a macroscopic substrate; (black) unenhanced Raman of a thick HKUST-1 layer used as a reference. Peaks labeled C−H(Ar) correspond to out-of-plane aromatic C−H bends. Reprinted with permission from ref 28. Copyright 2008 American Chemical Society.

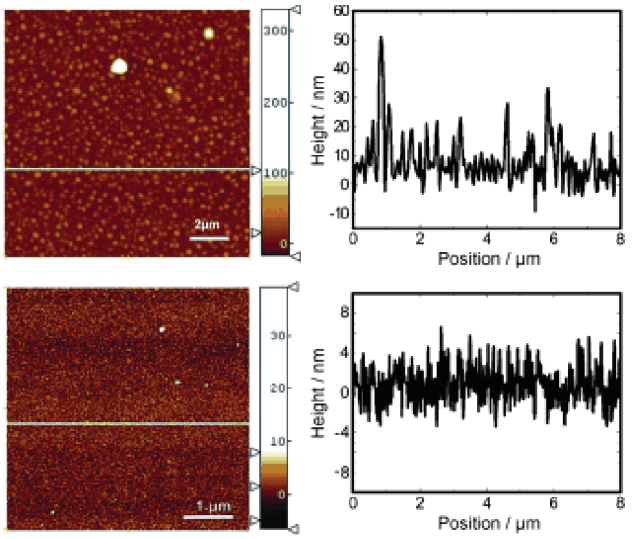

Figure 17. AFM images of $[Cu_2(ndc)_2(dabco)]$ SURMOFs. (Top) Twenty layers on a pyridine-terminated SAM (scale bar 2 mm, overall surface roughness around 16.1 nm). (Bottom) Twenty layers on a COOH-terminated SAM (scale bar 1 mm, overall surface roughness around 2.03 nm). Reprinted with permission from ref 72. Copyright 2011 Wiley-VCH.

dependence measurement consists of scanning the azimuthal angle Φ (rotation of the sample around its normal) at fixed θ and 2θ positions. No angular dependence was found, which suggested that the layers form uniformly without any preference in the direction of the substrate. The presence of misoriented crystallites may also be investigated by X-ray diffraction.[73] Indeed, when the MOF structure is tetragonal (e.g., in the case of $[Cu_2(ndc)_2(dabco)]$) a perfectly oriented film will exhibit only 00*l* lines in the out-of-plane mode and only *h*00 in the in-plane mode if the structure has been grown in the (001) orientation. The goniometer should subsequently be positioned at a Bragg peak position, for example, at 001 in the out-of-plane mode, and the sample stage should be moved to the in-plane geometry (χ angle at 90° from the other geometry) while recording the diffracted intensity. If disoriented crystallites are present, their (001) planes will be appear at a diffraction position at some point and the corresponding Bragg peak will appear. In the absence of disoriented crystallites, no feature other than the peak at the starting position will be recorded.

In some cases, integrated devices or small substrates are used and the substrate may not be sufficiently large for X-ray diffraction. In this case, Raman spectroscopy can be used. Indeed, Raman spectroscopy can be very efficient at assessing crystalline structure, particularly in the cases of ZrO_2 and CeO_2.[103] Allendorf et al.[28] coated microcantilevers with 20 cycles of HKUST-1, which were deposited by liquid-phase stepwise deposition. Prior to deposition, the microcantilevers were functionalized with gold and then with a SAM. The authors used microsurface-enhanced Raman spectroscopy (μSERS) to prove the identity of the MOF layer. This method relies on deposition of a thin (2.5 nm) silver layer on top of the MOF film, which greatly enhances the signal. An area of 2 μm^2 was demonstrated with the instrument. The identity of the film was proven by comparison of the film signal with the signal of a similar film grown onto a macroscopic surface (see Figure 16).

3.1.1.2. Morphology Studies. The study of thin films (20−40 nm) prepared from materials with low densities that are also insulators and sensitive to electron beams is not easily performed by scanning electron microscopy (SEM). Sputtering of the surface with a conductor, such as gold or carbon, is required for good resolution. In most cases, cross-section measurements of the thickness are not possible because the film cannot be clearly detected. The SURMOFs are much more conveniently studied by atomic force microscopy (AFM) or scanning force microscopy (SFM), which allows local study of the homogeneity and roughness of a SURMOF. HKUST-1 films grown by liquid-phase epitaxy are a good example: surface roughness was monitored as a function of the number of deposition cycles.[94] A 45-cycle HKUST-1 film grown in the [100] orientation on patterned COOH-/CF_3-terminated SAMs exhibited a surface roughness (root-mean-square, rms) of 5−6 nm over areas of up to 10 μm^2. Such a roughness corresponds to step heights of only two unit cells. When the substrate is patterned such that some locations are free from MOF film, measurements of the overall thickness of the film become possible. When applied on the aforementioned HKUST-1 film, such measurements gave direct evidence that after about 20 layers the growth mode is linear with an increase of one-half a unit cell per deposition cycle (metal + linker). Similar studies on $[Cu_2(ndc)_2(dabco)]$[72] (see Figure 17) and NAFS-1[67] SURMOFs also show low roughness and high lateral homogeneity.

3.1.1.3. Porosity Measurements. Most properties and potential applications of MOFs rely on their porosity. The pores should be easily activated (i.e., solvent molecules removed) and accessible to guest molecules. A common issue to any supported film is the thermal resistance. Indeed, when heated to high temperatures, films may develop cracks, due to the differences in the thermal expansion between the substrate and the film. The morphology may be greatly affected; delamination may occur. Consequently, low-temperature activation methods should be preferred: the solvent should be exchanged for a volatile one (typically chloroform or dichloromethane), and the film should be dried under a vacuum at room temperature or moderate temperature. Characterization of the porosity of polycrystalline films will be discussed in section 3.2. In the following sections, we will focus on the SURMOF case. The

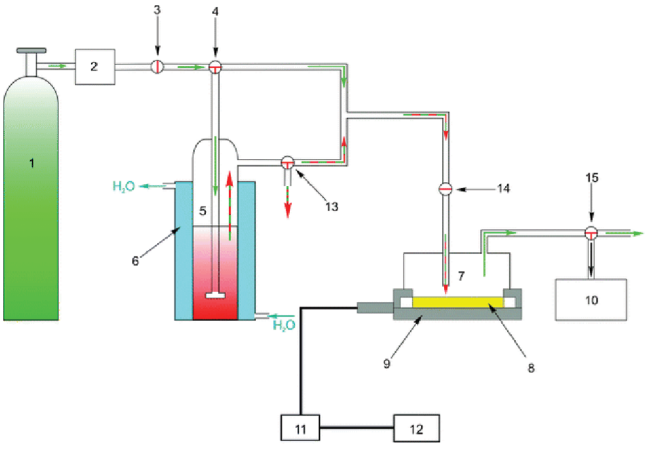

Figure 18. Setup employed for the sorption measurements: (1) argon supply, (2) gas flow controller (FMD PR4000), (3) main valve, (4) three-way valve, (5) storage container with the loading substance, (6) thermostat, (7) glass tube, (8) QCM sensor with gold electrodes, (9) sample holder with electric feed through, (10) membrane pump, (11) impedance analyzer, (12) PC, (13, 15) outlet valves, (14) inlet valve. Reprinted with permission from ref 27. Copyright 2010 PCCP Owner Societies.

small amount of deposited material must be taken into account: 20−40 nm thick porous films, spread over approximately 1 cm^2. In most cases, the thickness is not directly measured but rather is estimated from the number of deposition cycles or from XRD data. Shekhah et al.[69] coupled thickness measurements by AFM and BET surface area evaluations by krypton adsorption. Indeed, Kr adsorption allows a precise measurement of small surface areas. The obtained value of 627 ± 15 m^2 cm^{-3} is consistent with expectations from bulk MOF material. Nevertheless, this method is notably difficult to implement and requires a large amount of sample. Therefore, a more straightforward method was developed that is based on quartz crystal microbalance (QCM) equipment.

SURMOFs samples are fabricated under mild conditions (see section 2.1) and are thus compatible with sensitive QCM substrates. These substrates are usually covered with gold; they can be easily functionalized by a SAM and used as substrates for SURMOF growth. Biemmi et al.[21] introduced a setup for sample loading via the gas phase. A liquid analyte is kept at a constant temperature, and its vapors are dosed in a controlled evaporator mixer where they are mixed with a carrier gas (N_2) before reaching the QCM cell. The analyte sorption by the film is detected as a shift in frequency, translated to a mass uptake by the Sauerbrey equation,[104] and related to the weight of the activated film. Full water sorption isotherms were recorded on polycrystalline HKUST-1 films in this manner.

Because SURMOFs are thinner, smoother, and more homogeneous than polycrystalline films, more advanced studies are possible, such as determination of diffusivity values. Zyabalyo et al.[27] prepared a HKUST-1 SURMOF by LPE on QCM substrates. They used a simpler setup: the QCM cell received either a pure N_2 flow or an analyte-saturated flow (see Figure 18). The time dependence of the frequency change was recorded as the loaded gas entered the QCM cell. Frequency shifts were translated into mass uptakes and interpreted using a Fickian model of diffusion to obtain kinetic constants. Unfortunately, the chosen case (diffusion

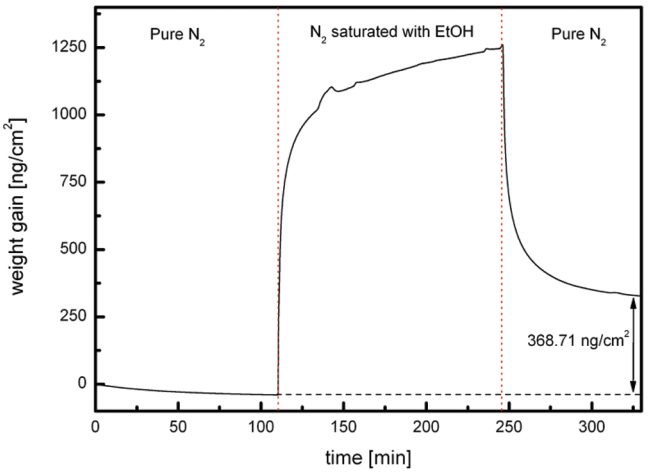

Figure 19. Ethanol uptake of a 40-cycle $[Zn_2(BME\text{-}bdc)_2(dabco)]$ SURMOF film.

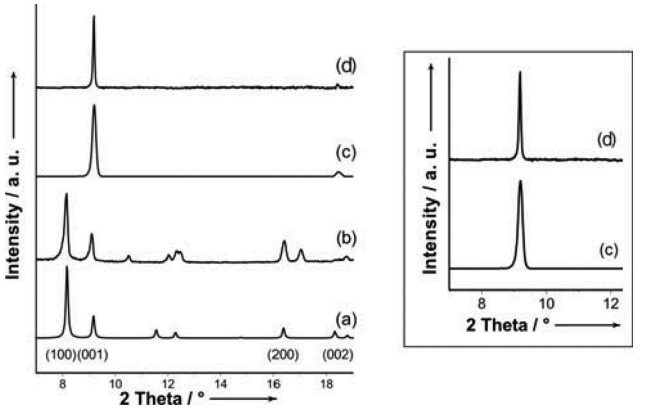

Figure 20. X-ray diffraction patterns (background corrected) of a 30-cycle $[Zn(BME\text{-}bdc)(dabco)_{0.5}]$ deposited on top of a 30-cycle $[Cu(ndc)(dabco)_{0.5}]$ MOF in [001] orientation on pyridine-terminated SAM (d) compared with the pattern of the 30-cycle $Cu(ndc)(dabco)_{0.5}$] MOF alone. Calculated patterns for bulk $[Cu(ndc)(dabco)_{0.5}]$ (a) and experimental data of bulk $[Zn(BME\text{-}bdc)(dabco)_{0.5}]$ (b) are included. Reprinted with permission from ref 72. Copyright 2011 Wiley-VCH.

of pyridine into HKUST-1) was not studied on bulk material; therefore, the diffusion constant, which was calculated to be 1.5×10^{-19} m^2 s^{-1}, could not be related to any other value. In addition, the diffusion constants that have been measured by various techniques in different MOFs differ from this value by several orders of magnitude.[105,106] Using a similar setup, we recently studied the gas-phase ethanol loading of the functionalized SURMOF $[Zn_2(BME\text{-}bdc)_2(dabco)]$ (BME-bdc = 2,5-bis(2-methoxyethoxy)-1,4-benzene dicarboxylate) (see Figure 19). A significant mass uptake was recorded when pure N_2 was switched to ethanol-loaded N_2. The uptake was first quick and then slower with a constant slope. When the system was switched back to pure N_2, part of the ethanol desorbed but a significant amount stayed. This amount corresponds to a loading of about 1.3 molecules per unit cell and is identical to the loading measured on powder (gas-phase loading of ethanol) by thermogravimetric analysis (TGA).[107]

3.1.2. MOF on MOF Heterostructures. Metal−organic frameworks are a subclass of coordination polymers and, as such,

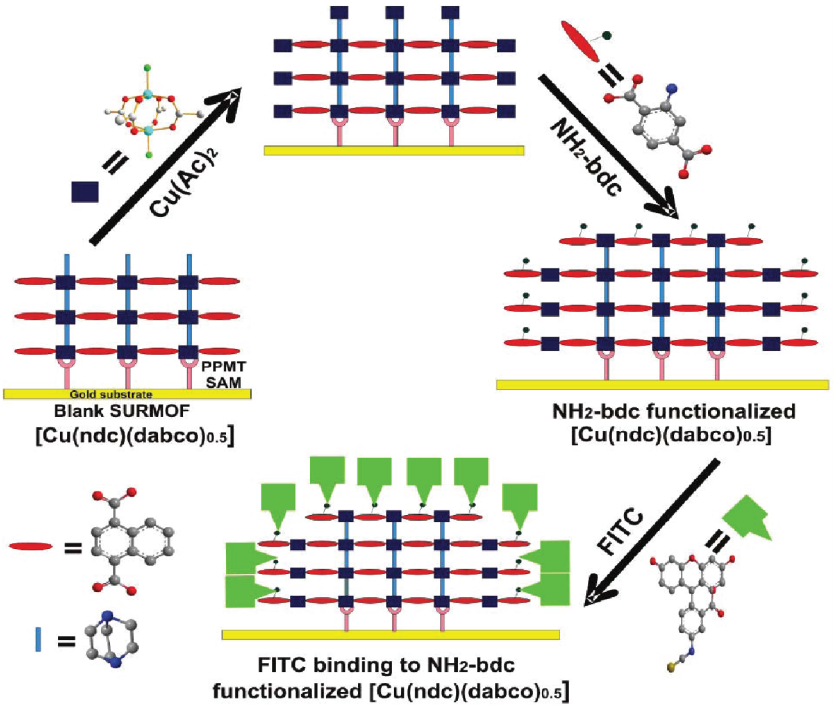

Figure 21. (Top) Stepwise approach for external surface functionalization of the preformed [001]-oriented SURMOF $[Cu_2(ndc)_2(dabco)]_n$ on pyridine-terminated SAM. (Bottom) Ligand exchange between acetate and NH_2-bdc and the reaction of NH_2-bdc with FITC. Reprinted with permission from ref 74. Copyright 2011 American Chemical Society.

members of the wide family of polymers. In agreement with block copolymers, several groups developed methods to grow MOFs on top of other MOFs in an epitaxial fashion.

The first example of core−shell MOF single crystals was published by Kitagawa and co-workers.[7] They started from $[Zn_2(ndc)_2(dabco)]$ single crystals approximately 200 μm in size and immersed them in a solvothermal mother solution for synthesis of $[Cu_2(ndc)_2(dabco)]$. Hybridized core−shell crystals were harvested in high yields. Advanced XRD analyses indicated that the shell was also a single crystal and that it was grown epitaxially at the surface of the core crystal, with a small rotation angle for lattice mismatch accommodation. Koh et al.[8] expanded this work by growing ABA-type hybridized crystals based on MOF-5 and IRMOF-3. This last work is particularly interesting because the two MOFs, A and B, differ in their functionality that is borne by the organic linker (bdc in the MOF-5 case, NH_2-bdc in IRMOF-3). The path to multifunctional MOF materials is thus open and, of course, of great interest to researchers involved in MOF films.

SURMOFs are particularly well suited for multilayered architectures because of their high degree of crystalline order and orientation, smoothness, and versatile synthesis methods. Proofs of principle were first given by Zacher et al.[72] The functionalized SURMOFs ($[Cu_2(F_4bdc)_2(dabco)]$ and $[Zn_2(BME\text{-}bdc)_2(dabco)]$) were grown on top of $[Cu_2(ndc)_2(dabco)]$ SURMOFs. The high degree of crystallinity and orientation of the bottom layer was maintained after the top layers were added. Because of the same topology and similar cell parameters of the different MOFs, the diffraction lines from the different MOFs occur at the same positions. Nevertheless, the broadness of the line was reduced and the overall thickness calculated from single-line analysis fitted well to the overall number of deposition cycles (see Figure 20). Such multilayered SURMOFs are, however, difficult to characterize precisely. Indeed, it is not possible to perform typical depth-profile experiments by X-ray photoelectron spectroscopy (XPS) because Ar-ion sputtering induces a strong intermixing of the SURMOF layers. The question of the interface between two SURMOFs is thus still open. Shekhah et al.[73] recently used advanced XRD techniques (detailed in section 3.1.1.1) in a synchrotron facility to characterize the degree of orientation of a $[Zn_2(ndc)_2(dabco)]$ SURMOF grown on top of a $[Cu_2(ndc)_2(dabco)]$ SURMOF. The results indicate a perfect orientation in the (001) direction and the absence of disoriented crystallites, both in the bottom SURMOF and in the resulting heterostructure. A particularly interesting application of the MOF-on-MOF heterostructure concept would be the possibility to "protect" a water-sensitive SURMOF from moisture by growing a hydrophobic SURMOF on top of it, such as by using a fluorine-containing linker.

3.1.3. Surface Modification of SURMOFs. Well-defined objects, such as MOF single (macro) crystals and SURMOFs, are good candidates for selective modification of their *external* surfaces or crystallite facets. Surface modifications of MOF single crystals were pioneered by Gadzikwa et al.,[108] who were inspired by postsynthetic modification strategies. A reactive group was incorporated into the ligand and protected so as to allow synthesis of MOF single crystals. The ligand was then deprotected and subjected to a Cu(I)-catalyzed click chemistry reaction with a long polyethylene glycol (PEG) chain. The sizes of the deprotecting agent and polymer were thought to prevent them from penetrating the MOF structure. The surface properties were indeed tuned: the surface was transformed from hydrophobic to hydrophilic. Kondo et al.[109] recently demonstrated a more simple,

one-pot approach for face-selective decoration. A well-known dye, BODIPY, was modified to bear carboxylic acid moieties. Single crystals of $[Zn_2(ndc)_2(dabco)]_n$ were immersed in a modified BODIPY solution for 3 h at 45 °C. A ligand exchange reaction occurred between the ndc ligands that terminate four of the cubic crystal faces and the modified dye molecules, which are too bulky to enter the pores of the structure. Fluorescence was detected by confocal laser scanning microscopy: the COOH-terminated faces were all fluorescent, which confirmed the ligand-exchange reaction. In the case of HKUST-1 crystals that contain only COOH-based coordination bonds, the entire surface of the crystals became fluorescent.

A related approach has been applied for external surface modification of SURMOFs,[74] which is schematically described in Figure 21. A dye (FITC) bearing an isothiocyanate moiety was grafted onto NH_2 surface groups. Unfortunately, achieving good-quality $[Cu_2(ndc)_2(dabco)]_n$ SURMOF by use of amino-functionalized terephtalic acid (NH_2-bdc) instead of ndc is difficult. Therefore, a $[Cu_2(ndc)_2(dabco)]_n$ SURMOF that is inert to FITC was first prepared. During the last cycle, the mixture of the ndc and dabco solutions that was used for growth (see section 2.1) was substituted with a solution of NH_2-bdc. Thus, only the external surface of the SURMOF was functionalized with NH_2 groups. In a second step, the SURMOF was placed into contact with a solution of FITC (and a base). The samples were observed under a fluorescence microscope, and a strong fluorescence was detected, which indicated successful grafting of FITC molecules. Samples that were not functionalized by NH_2-bdc showed little or no fluorescence. After deposition of two inert layers (bdc or ndc instead of NH_2-bdc) on top of the NH_2-bdc-modified SURMOF, binding of FITC was quantitatively suppressed. This finding agrees with the surface roughness of the initial SURMOF being approximately ±1 layer. Essentially, these experiments point to the unique possibility of deriving a layer-selective functionalization of SURMOFs within the bulk of the film under optimum conditions.

3.2. Polycrystalline Films

3.2.1. Characterization. Characterization of MOF polycrystalline films is essentially similar to SURMOFs but more straightforward, mainly because of their greater thicknesses. Standard X-ray diffraction is the main tool used to assess the structure in the out-of-plane mode by comparison with powder references. Even if AFM can provide useful information, SEM is more commonly used to observe the morphology and measure the thickness. The porosity is rarely assessed by gas adsorption measurements, even in the case of thick films. Nevertheless, indirect tools, such as loading with probe molecules (e.g., metallocene derivatives[42,75]), vapor sensing,[21,23] environmental ellipsometry,[50] or gas separation[51,57] assess the accessibility of the pores.

3.2.2. Controlling the Microstructure. Obtaining the desired microstructure or morphology may be difficult during preparation of a MOF film. When performed by direct synthesis in a mother solution, the nucleation rate may be too low at the surface and the resulting film will not be continuous. In this case, it may be helpful either to change the synthesis conditions or solvent, although such changes are not always possible, or to change the synthesis method to, for example, seeded growth. The works of Bux et al.[51] and McCarty et al.[55] on ZIF-7 and ZIF-8 films illustrate an important point: additives in the synthesis mixture can help control the microstructure of the

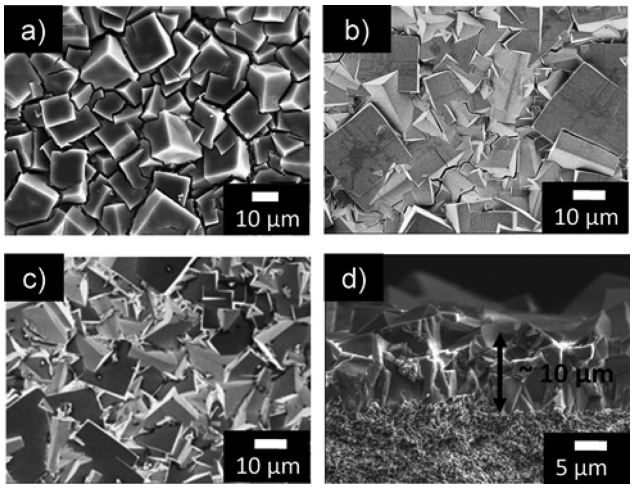

Figure 22. SEM images of IRMOF-3 membranes after drying (a) without surfactant, (b) with a triblock copolymer, P-123, and (c) with Span 80. The cross-sectional view (d) is from the membrane dried in the presence of Span 80. The thickness of the membrane is ~10 μm. Reprinted with permission from ref 78. Copyright 2011 American Chemical Society.

film. In both cases, sodium formate was used as a basic additive. In the postulated mechanism,[55] small ZIF-8 crystals are terminated with neutral 2-methylimidazole linkers. Sodium formate increases the synthesis pH and enables full deprotonation of the linkers, which allows crystal growth to proceed in all directions. Such reactions yield large crystals rather than the branched structures that are usually observed. As a result, the crystals at the surface are large and well intergrown instead of being small and scattered at the surface. This idea is strongly related to the field of nano-MOFs and the surface chemistry of MOFs and is also relevant for preparation of seeds for seeded growth. A detailed discussion of this topic is beyond the scope of this review; more information can be found elsewhere.[17,99]

Formation of cracks upon cooling the film (when deposited from the reaction mixture), upon activation (solvent exchange and/or drying), or upon aging (if the sample is water sensitive, for example) is also undesirable. To avoid formation of cracks upon cooling, the film should be cooled slowly and, if possible, while still immersed in its mother solution. Cracks are more likely to occur upon drying. Solvent exchange for low-boiling solvents, such as methanol, chloroform, or dichloromethane, is beneficial because the film can then be activated without being subjected to high temperatures. Another common method to avoid cracking is to dry the films under nearly saturated conditions. The films are placed in an oven next to a beaker filled with solvent and gently heated for sufficient time (typically a few days). This approach proved successful for HKUST-1[31,38] and IRMOF-3,[78] for example, even if the samples were only partially dried.

Aging is a problem when the MOF degrades in air, and this problem is particularly notable for the famous IRMOF-*n* family. These materials have interesting properties that have been well studied in the bulk phase, but few applications as films have been presented because of their water sensitivity. Yoo et al.[78] prepared air-stable, crack-free IRMOF-3 membranes using a surfactant-assisted drying method. IRMOF-3 membranes were prepared in DMF following a procedure described in section 2.2.2.3. The

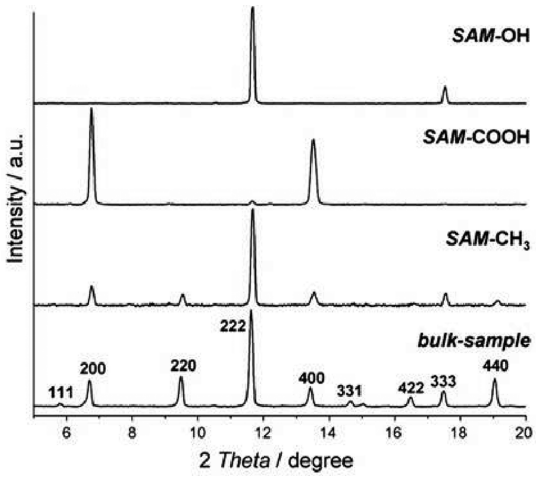

Figure 23. X-ray diffraction patterns (background corrected) of thin films of HKUST-1 on functionalized gold surfaces compared with the pattern of a randomly oriented HKUST-1 powder sample. Each pattern is normalized to the most intense reflection. Reprinted with permission from ref 20. Copyright 2007 American Chemical Society.

films were immersed for 3 days in chloroform to exchange DMF occluded in the pores. They were then immersed in a chloroform solution containing a surfactant, Span 80 (sorbitan oleate, $C_{24}H_{44}O_6$), and dried at room temperature under nearly saturated conditions. SEM images (see Figure 22) demonstrated a clear improvement in the morphology. The film turned hydrophobic and was crack free and stable for more than 1 month, whereas a membrane that did not contain a surfactant was stable for only a few hours. The authors also showed that the presence of the surfactant somewhat reduces the apparent BET surface area, but it efficiently protected the membrane from degradation in air.

3.2.3. Controlling the Orientation. The orientation of a MOF thin film is particularly important for applications that require mass transfer through the film and where the MOF has 1D or 2D pores. The porosity or channels should thus be oriented, in the best case, perpendicularly to the substrate or at least with a sufficiently high angle. Several examples have been published where the MOF film grows "naturally" oriented upon deposition[64] or retains the preferential orientation of its seeding layer.[45,70] However, in most cases, the films are obtained either randomly oriented or even sometimes wrongly oriented (1D pores lying parallel to the substrate). Several groups have shown that additives or carefully chosen precursors can help to obtain a desired orientation. For example, replacement of formic acid by sodium formate for synthesis of $[Mn(HCOO)_2]$ on porous alumina transformed the channel from being preferentially parallel to the substrate to an angle of 34° relative to the surface.[79] In other cases, addition of a base[58] or a change of the solvent[82] can trigger oriented growth from a randomly oriented seeding layer. The explanation for such behaviors is related to the nature and activity of growth species in solution, which can be influenced by the pH or solvent of the mother solution. The study by Li et al.[58] that involved fabrication of oriented ZIF-7 membranes is particularly interesting. The authors showed that the aspect ratio of ZIF-7 crystals in solution (i.e., the ratio of the average crystal length to the average crystal width) can be controlled using zinc chloride instead of zinc nitrate as a precursor and varying the amount of diethylamine added as a deprotonating agent. The randomly oriented seeding layer was deposited by dip coating into a colloidal solution of ZIF-7 seeds and polyethylene imine. The seeds were nearly spherical. For secondary growth, optimized conditions for synthesis of thin microrods were used and allowed formation of a 2 μm thick film made of well-intergrown columnar grains with the *c* axis slightly tilted (10°) from the normal to the surface.

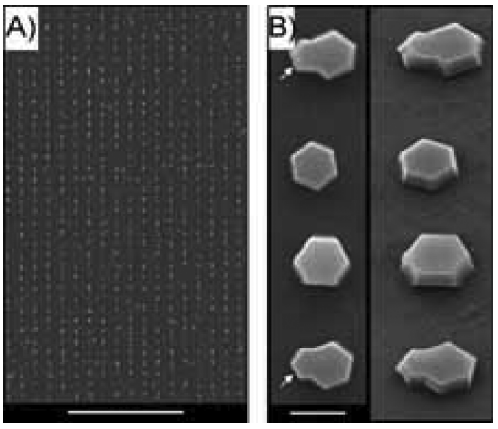

Figure 24. Patterned deposition of HKUST-1 crystals: (A) scale bar 25 mm. (B) Details of individual crystals viewed from above (left) and at a 35° angle (right): scale bar 1 mm. Arrows indicate intergrowths caused by a second nucleation. Reprinted with permission from ref 33. Copyright 2010 Wiley-VCH.

Another approach relies on the use of self-assembled monolayers (SAMs) to direct growth. Bein and co-workers studied growth of MOFs, such as HKUST-1,[20] on SAM-modified substrates by direct growth from preconditioned mother solutions at room temperature (see section 2.2.1.2.). They observed different orientations that depended on the functionality of the SAM (COOH, OH, or CH_3 terminated): COOH-terminated SAMs favored orientation along the [100] direction (pyramid-shaped crystals), and OH-terminated SAMs favored [111] orientation (octahedral crystals) (see Figure 23). Using either direct growth from the mother solution at room temperature or gel-layer methods, Fe-MIL-88B,[85] Fe-MIL-88B-NH_2,[30] and CAU-1[81] were also obtained as perfectly oriented films on top of COOH-terminated SAM, whereas OH-terminated SAMs led to less-strongly oriented films.

The SAM alone, however, is not always sufficient to explain orientation. The synthesis conditions also play a critical role, as exemplified by HKUST-1. Schoedel et al.[30] used gel-layer synthesis and obtained [111]-oriented crystals independently of the SAM. Zacher et al.[18] performed growth under solvothermal conditions (see section 2.2.1.1) and obtained [111]-oriented crystals on a COOH-terminated, silane-based SAM. Ameloot et al.[33] deposited crystals on variously functionalized surfaces by evaporation-induced crystallization (see section 2.2.1.5) and always observed the same [111] orientation. Zhuang et al.[41] precipitated MOF crystallites by solvent vapor diffusion and also observed only [111] orientation (see section 2.2.1.2).

3.2.4. Controlling the Spatial Localization/Functionality. The ability to control the spatial repartition of a functional material on a surface is of key importance in many applications, which is why patterning techniques are becoming more important.

Use of SAM-modified substrates allows an easy spatial functionalization by microcontact printing. The method is relatively cheap and quick and allows sufficient precision. For

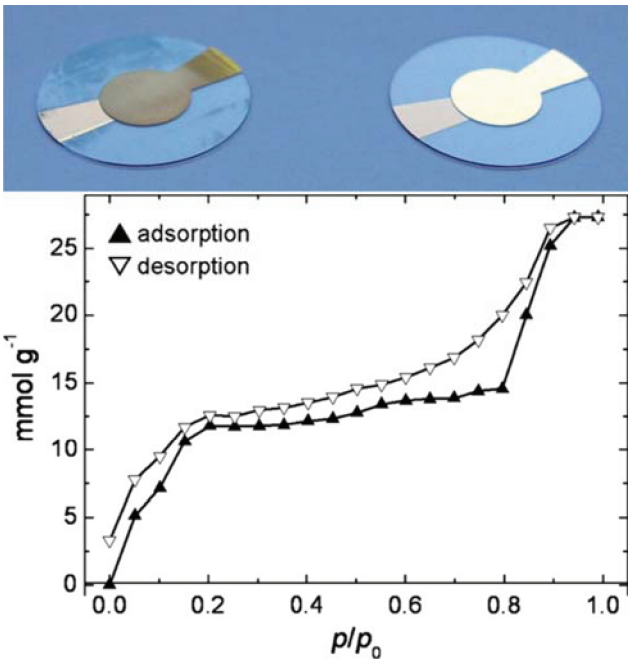

Figure 25. (Top) QCM devices after growth of $[Cu_3(BTC)_2(H_2O)_3 \cdot xH_2O]$: opaque layer on the SAM-modified gold electrode (left); reference chip without SAM on the gold surface (right). (Bottom) Water sorption isotherm of a thin film of $[Cu_3(BTC)_2]$ recorded at 294 K with the QCM setup. Reprinted with permission from ref 21. Copyright 2008 Elsevier.

example, it has been shown that many MOFs do not grow on CF_3-terminated SAMs[18,42] (either thiol or silane based), whereas they do grow on COOH- or OH-terminated SAMs. In the case of a thiol-based SAM, such films cannot be used at elevated temperatures (typically above 80°). Yet SAMs that contain covalent Si—O—M (M = surface atom) bonds can withstand much higher temperatures, often temperatures that are above the decomposition temperature of many MOFs, and can be patterned as well. Gassensmith et al.[110] recently demonstrated that microcontact printing of silane-based SAMs is indeed compatible with direct synthesis in a mother solution at 85 °C.

Ameloot et al.[33] also used microcontact printing to control the spatial repartition of MOF crystallites at the surface. They inked a patterned PDMS stamp with a clear MOF mother solution (see section 2.2.1.5 for details) and applied it to a surface. Because the liquid was confined between the stamp and the substrate, MOF crystallites formed only under the stamp, Figure 24.

When metallic substrates are used, well-known methods used in the electronics industry can be applied, such as metal evaporation under a mask. A good example is the report by Ameloot et al.[24] The authors started from a glass slide treated with chlorotrimethylsilane. This surface is improper for MOF growth because the solvent does not wet the surface. Copper was subsequently evaporated on the substrate in a pattern (see Figure 13). The MOF growth solution (a mixture of btc linker and silver nitrate) was spin coated onto the glass slide. Because of silane treatment, the MOF growth solution was confined to the copper squares and so was the resulting MOF film.

The seeded growth method also enables, in some cases, control of the spatial localization of the film. A good example is the work of Falcaro et al.,[48] who dropped the seed solution onto only a part of the substrate. After drying, the substrate (alumina or silicon wafers) was immersed into a MOF-5 synthesis solution in *N,N*-diethylformamide (DEF) and incubated at 95 °C for 12 h. Interestingly, MOF crystals were formed only in the regions covered with seeds and not elsewhere. This method is simple; it requires only that seeds are strongly attached to the substrate such that they do not migrate during the secondary growth step. The method is particularly efficient when the heterogeneous nucleation rate of the MOF on bare substrates is low.

4. APPLICATIONS OF MOF FILMS

4.1. Overview and Comments on Substrates

On the basis of the collection of literature in Table 1, a large diversity of substrates can be coated with MOF films, such as metals, oxides, polymers, and textiles, for example, irrespective of the smoothness, roughness, or porosity of the substrate. Often, the substrate is determined by the intended application. However, in many cases, the substrate will determine the deposition technique or at least reduce the number of viable choices. Indeed, integrated, patterned, or sensitive devices will probably not withstand high temperatures or corrosive acidic solutions, and control over the spatial localization may be lost (see section 3.2.4). Therefore, only "soft", low-temperature methods must be used. For nonsensitive substrates with complicated shapes, such as catalytic beads (made of alumina), tubular porous alumina, and pulp fibers, direct synthesis under solvothermal conditions or stepwise deposition gives the best results.[32,37,48,65,66] In cases where the nucleation rate at the surface is insufficient, some of the strategies discussed in section 2.2, such as surface modification by organic linkers or seeded growth, may be helpful.

4.2. Sensing Applications

The unique combination of properties found in metal—organic frameworks makes them interesting for applications as sensors. Indeed, large surface areas combined with an appropriate tuning of the pore structure and chemical functionality suggest that high analyte sensitivity and selectivity could be achieved. Several transduction mechanisms are possible, including luminescence, changes in optical properties, use of quartz crystal microbalances, use of microcantilevers, and changes in electrical properties. This last transduction mechanism is not currently possible because it would require networks that are not insulators (and, to date, almost all MOFs are insulators). A few proofs of principles are now in the literature and will be reviewed here. A detailed discussion on transduction mechanisms and considerations that should be made when selecting or designing a MOF for detection is beyond the scope of this review and can be found elsewhere.[9]

4.2.1. QCM-Based Sensors. One of the most straightforward approaches to devising a sensor is to use quartz crystal microbalance (QCM) equipment. Indeed, typical substrates for such devices are quartz plates coated with a material such as gold, silica, or copper. Thus, many growth methods described in section 2 are compatible with QCM substrates as soon as they take place at low temperature. After a QCM substrate is appropriately coated, adsorption and desorption of molecules can be easily monitored by recording the change in the oscillation frequency of the substrate; the sensitivity is usually in the nanogram range and thus adapted to thin films.[111] Biemmi et al.[21] performed the first detailed study of water sorption in an HKUST-1 film grown directly on SAM-modified gold QCM electrodes. To grow the film, SAM-modified QCM substrates were immersed in an HKUST-1 mother solution at room temperature (see section 2.2.1.2 for details) to form an opaque

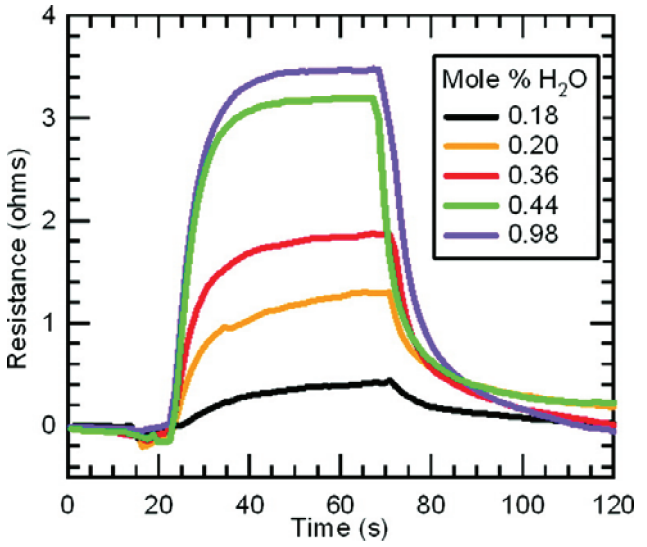

Figure 26. Temporal response of the cantilever piezoresistive sensor to water vapor diluted in N_2 (room temperature, 1 atm). Reprinted with permission from ref 28. Copyright 2008 American Chemical Society.

layer, as shown in the top of Figure 25. The substrates were then installed in the QCM setup and exposed to different concentrations of water vapor. The weight of the water adsorbed into the film was detected as a frequency shift, which was translated into a mass uptake using the Sauerbrey equation[104] and related to the mass of the empty film. Complete water sorption isotherms were thus recorded (Figure 25, bottom). Interestingly, the amount of water adsorbed at $p/p_0 = 0.8$ was approximately 16 mmol g^{-1}, i.e., identical to the amount of water contained in a bulk HKUST-1 sample exposed to an atmosphere of 80% relative humidity at the same temperature, as measured by thermogravimetric analysis (TGA). The water sorption isotherms obtained by the QCM-based method are thus consistent with bulk results.

Because water sorption is of general interest in the field of humidity sensing, several other groups have tested MOFs for this purpose. For example, Ameloot et al.[23] synthesized HKUST-1 coatings by electrochemical deposition directly on top of QCM substrates and studied the response toward gas flows of increasing relative humidity. Water uptake of the film was measured is a manner similar to the previously described case. In addition, the authors observed a high reproducibility of the signal upon sequentially cycling dry and water-containing nitrogen flows.

4.2.2. Stress-Induced Chemical Detection. Allendorf et al.[28] also chose HKUST-1 as a test MOF for a microcantilever-based sensor system. Indeed, upon inclusion of molecules in the pores, the lattice parameters of the MOF may expand or shrink as a consequence of the attractive or repulsive interactions between the host molecules and the guest framework. This creates mechanical stress at the interface between the MOF film and its substrate, which that can be detected if the substrate is a microcantilever because the mechanical stress induces its bending. This approach allowed the authors to fabricate a responsive, reversible, and selective sensor for water (see Figure 26), methanol, and ethanol vapors, whereas N_2 or O_2 triggered no answer. HKUST-1 films on microcantilevers were fabricated using either liquid-phase stepwise deposition or direct growth in a mother solution at room temperature (after Biemmi et al.[20]). Prior to both methods, the microcantilevers were first coated with gold and functionalized with a SAM.

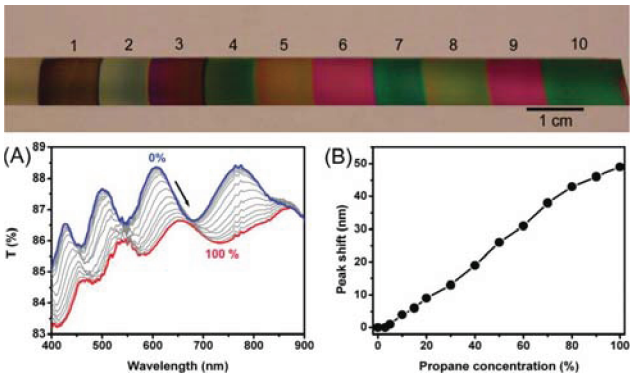

Figure 27. (Top) Photograph of a series of ZIF-8 films of various thicknesses grown on silicon substrates. (Bottom) (A) UV−vis transmission spectra of a 10-cycle ZIF-8 film grown on a glass substrate after exposure to vapors of ethanol and water. (B) Interference peak (originally at 612 nm) shift versus ethanol concentration in ethanol/water solutions. The concentration is expressed as a volume percentage. Reprinted with permission from ref 49. Copyright 2010 American Chemical Society.

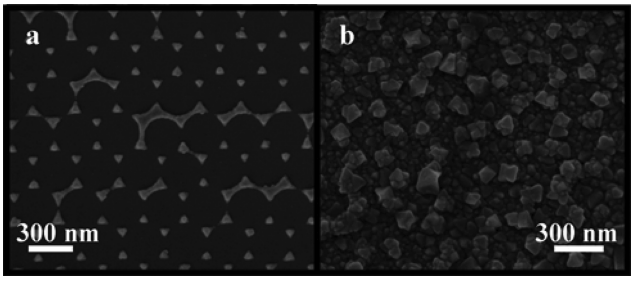

Figure 28. SEM images of (a) a triangular Ag nanoparticle array fabricated by nanosphere lithography on a glass coverslip and (b) a Ag nanoparticle array coated with 20 cycles of polycrystalline HKUST-1 film. Reprinted with permission from ref 29. Copyright 2010 American Chemical Society.

4.2.3. Devices Based on Optical Properties. Variations of optical properties (color, refractive index) are commonly used in the sensing field. Lu and Hupp[49] recently demonstrated that the apparent color of a MOF film may be determined by its interference properties. The authors grew micrometer-thick homogeneous ZIF-8 films on a silicon substrate by repeatedly immersing the substrate in a freshly prepared mother solution (see section 2.2.1.3 for details). The films are colorless, but when they are applied on a colored substrate, they display different colors as a result of thickness-dependent constructive and destructive interferences within the film, as shown in Figure 27. This effect can be precisely quantified by UV−vis spectra when the films are deposited on glass substrates. Fabry−Pérot fringes appear, and their maxima are shifted when an analyte diffuses into the films and undergoes a change in its optical constant. A detailed study was performed with a 1 μm thick film and propane as the analyte. A nearly linear peak shift occurred when the propane concentration was increased (see Figure 27).

When fabricating MOF films by the assembly of preformed colloids (see section 2.2.4), the packing degree is able to influence the overall refractive index. This index is also influenced by the swelling/contracting of the film (in cases where a flexible MOF has been used) or by the solvent filling the pores. MOF

Table 2. Selected Examples of MOFs for Sensing Applications[a]

MOF formula	analytes	mechanism	detection	refs
$[Zn_2(bdc)_2(dpNDI)]$	mono- and disubstituted aromatics	NDI−guest interactions	shift in emission wavelength	113
$[Zn_2(bpdc)_2(bpee)]$	explosives (DNT, DMNB)	quenching of linker fluorescence	luminescence quenching	114
$[Ln_2(HFIPBB)_3]$	ethanol	coordination to Ln^{3+}	luminescence quenching	115
Zn-1,2,4,5-ben- zenetetracarboxylate doped with Eu^{3+} or Tb^{3+}	Cu^{2+}, Co^{2+}	replacement of Ln^{3+}	quenching of lanthanide luminescence	116
$Zn_4O(SDC)_3$	high energy protons and alpha particles	linker luminescence	light emission	117
FeBTC	ethanol, methanol, water	interactions with framework	impedance sensor	118
$[Fe(pz)Ni(CN)_4]$	acetonitrile	adsorption in framework	color change (spin state change)	119
$[Cu_3(PTMTC)_2]$	ethanol, methanol	adsorption in framework	change in magnetic response	120

[a] dpNDI = *N*,*N*′-di(4-pyridyl)-1,4,5,8-naphthalenediimide, bpdc = 4,4′-biphenyldicarboxylate, bpee = 1,2-bipyridylethene, HFIPBB = 4,4′-(hexafluoro-isopropylidene)-bis(benzoic acid), SDC = stilbene dicarboxylate, PTMTC = polychlorinated triphenylmethyltricarboxylate.

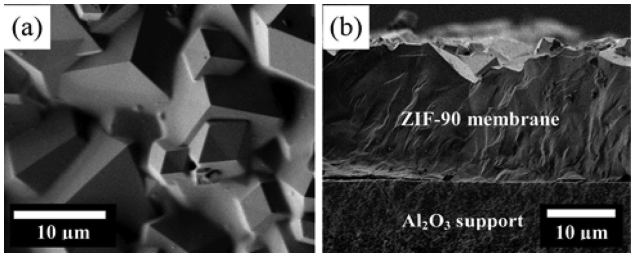

Figure 29. (a) Top view and (b) cross-section SEM images of the ZIF-90 membrane supported on the APTES-modified Al_2O_3 support. Reprinted with permission from ref 62. Copyright 2010 American Chemical Society.

films were studied using environmental ellipsometry;[112] with this technique, the optical index and thickness of the film can be monitored in situ in a controlled atmosphere containing gas or vapors at a chosen concentration. ZIF-8 was chosen for the test experiments because it exhibits a high affinity for organic solvents over water. Mixtures of isopropanol and water were subsequently fed to the sample, and a significant level of adsorption (and thus a change in refractive index) was recorded from a 1% solution of isopropanol in water.[50]

Fluorescence quenching has also been demonstrated[89] with the MOF $[Zn_3(btc)_2]$. When immersed in a diethylamine solution, the fluorescence intensity of the MOF decreases but not linearly with increasing analyte concentration. Other analytes, such as methanol, acetone, or aniline, trigger no response. However, to be applicable as thin films, strong fluorescence emitters are required, which makes this mechanism less interesting than others.

In most works, the MOF has been used as a sensor in itself, both adsorbing the analyte and providing a detectable response. In an interesting contribution, Kreno et al.[29] have shown how a MOF can be coupled with an already existing, nonselective sensor device to improve its selectivity. Here, the response is provided by silver nanoparticles. Very small changes in the refractive index of bulk silver can be detected using localized surface plasmon resonance (LSPR). Such changes may be caused by the accumulation of certain gaseous molecules around the nanoparticles. By selectively storing one type of gas molecule, a MOF coating around the nanoparticle can greatly enhance the signal. On their array of Ag nanoparticles, the authors grew a

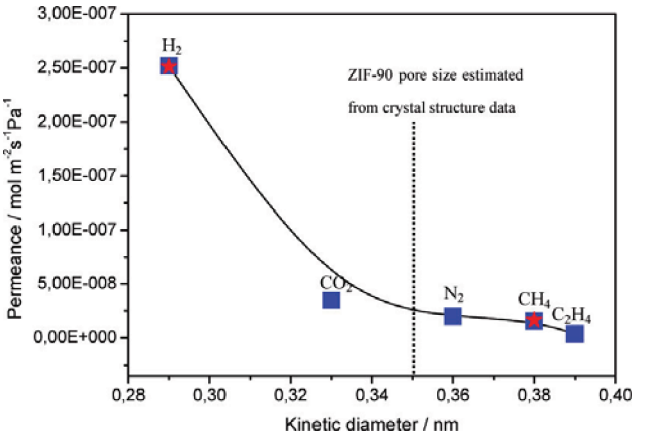

Figure 30. Single-gas permeances of different gases on the ZIF-90 membrane at 200 °C as a function of their kinetic diameter. The pentacles show the permeances of H_2 and CH_4 from an equimolar binary mixture. Reprinted with permission from ref 62. Copyright 2010 American Chemical Society.

coating of HKUST-1 by liquid-phase epitaxy (see Figure 28). The nanoparticles were first functionalized with a COOH-terminated thiol-based SAM.

Because HKUST-1 is able to adsorb large amounts of CO_2, this gas was chosen as the analyte. The influence of the coating thickness was investigated, and 37 cycles of deposition was found to be optimal. X-ray diffraction confirmed the crystallinity of the MOF thin film, and a 14-fold enhancement of the sensing signal was observed. The signal could be successfully calibrated with respect to the concentration of CO_2 into a N_2 flow. The significant advantage of this method is its versatility: it is not specific to a single MOF or to a single analyte; different sensing devices for different gases could easily be built using other MOFs that are selective to other analytes.

4.2.4. Other Mechanisms. Liu et al.[36] recently demonstrated the possibility for MOF films to be used as capacitive humidity sensors. The same group first realized a HKUST-1 membrane supported on a copper net (section 2.2.1.1 and Figure 3); in their study, they used a copper slice as the substrate (and electrode) and deposited circular aluminum electrodes on top of the film by evaporation under vacuum with a mask. The capacitance of the

dx.doi.org/10.1021/cr200167v |*Chem. Rev.* 2012, 112, 1055–1083

film was measured under various relative humidity conditions, and a linear response of ΔC was observed upon variation of the relative humidity. Furthermore, the measurements exhibited good reproducibility and good stability over time.

A number of other transduction mechanisms have been considered for sensing with MOFs, although they have not been applied to films. Table 2 presents a few examples of MOFs that are representative of various analyte−framework interactions along with the detection mechanisms for which proofs of principle have been established. A method of processing such MOFs as thin films would be of great interest for the development of MOF-based sensing devices.

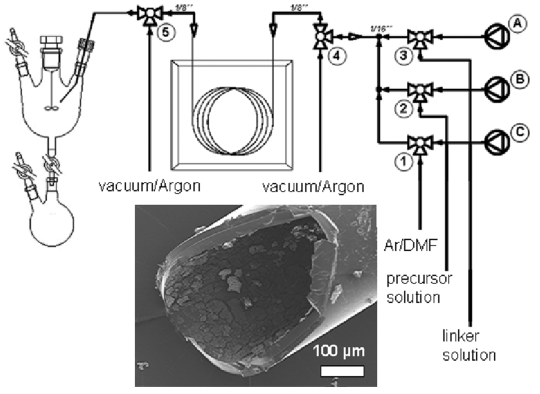

Figure 31. Setup for the automated preparation of MOF-coated fused-silica GC capillaries. Computer-controlled syringe pumps for application of the precursor, linker, and rinsing solution are denoted by A, B, and C, respectively. The three-way (1−5) valves allow the refill of the syringes, flushing of the capillaries with argon, and evacuation of the whole apparatus. Adapted with permission from ref 47. Copyright 2011 Wiley-VCH.

4.3. Separation

4.3.1. Membrane-Based Separation. Chemical separation in MOFs is based on two concepts: adsorption-based methods and kinetic separation. In the first case, bulk MOFs are used as adsorbents to store certain molecules.[121] Kinetic separation can be achieved by packed beds or, more conveniently, by use of

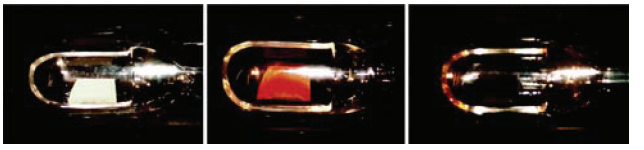

Figure 33. Optical images (digital photographs) of an empty 5 μm thick MOF-5 thin film on sapphire substrates before (left) and after (middle) their exposure to the vapor of the deep-red MOCVD precursor $[(\eta^5\text{-}C_5H_5)Pd(\eta^3\text{-}C_3H_5)]$. Subsequent treatment of the loaded film with UV light converts $[(\eta^5\text{-}C_5H_5)Pd(\eta^3\text{-}C_3H_5)]$@MOF-5 into Pd@MOF-5, which is visible by the color change to deep black (right). Reprinted with permission from ref 43. Copyright 2007 American Chemical Society.

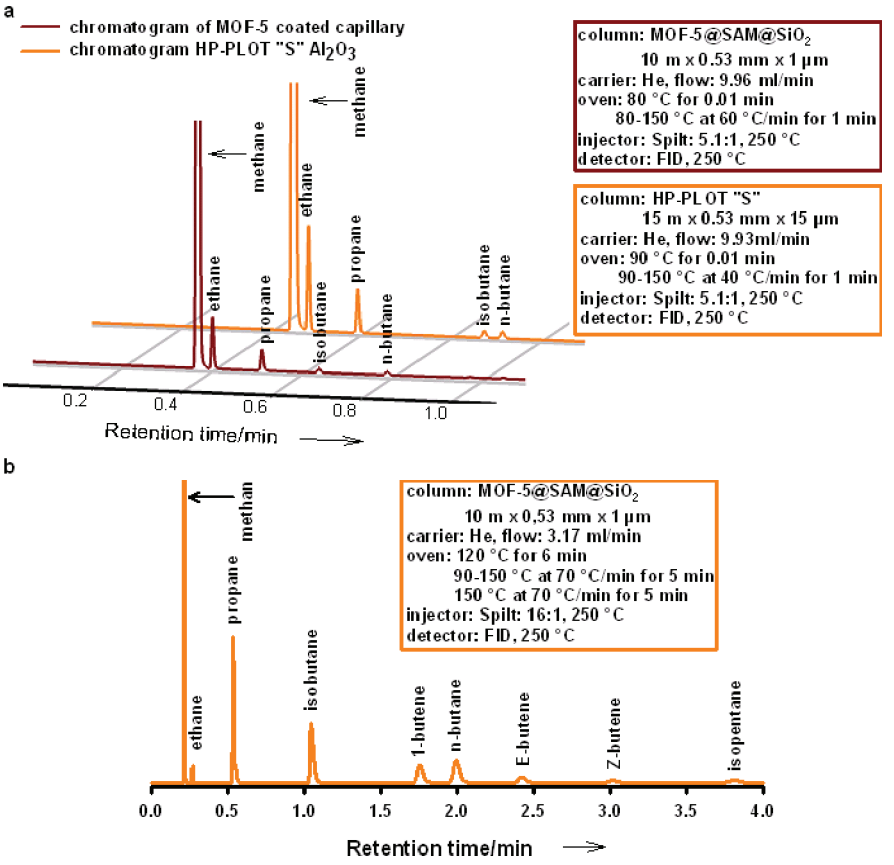

Figure 32. (a) Comparison of two chromatograms of natural gas (Freiberg, Germany, April 2010) obtained from the MOF-5-coated column (brown line) of Figure 2 and a Al_2O_3-based, Na_2SO_4 deactivated commercial PLOT column (Agilent HP-PLOT "S") (orange) optimized with respect to full basis separation and shortest retention time. (b) Chromatogram of a sample containing a mixture of natural gas and commercially available butane gas.[47] Reprinted with permission from ref 47. Copyright 2011 Wiley-VCH.

dx.doi.org/10.1021/cr200167v |Chem. Rev. 2012, 112, 1055–1083

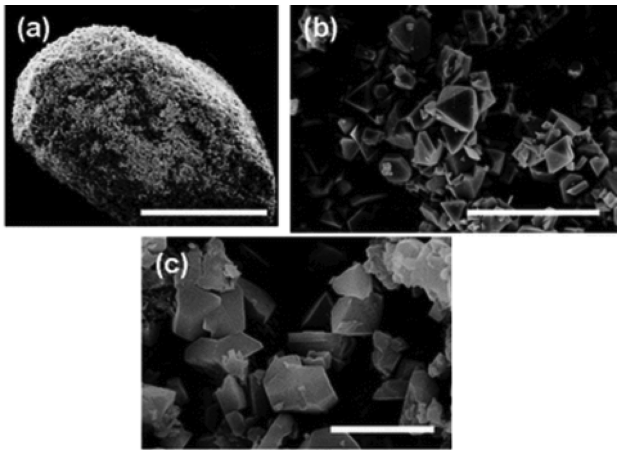

Figure 34. SEM data of an HKUST-1@PAM_1.0 composite prepared under solvothermal conditions. (a) SEM of a single-composite bead; scale 1 mm. Cross section of a bead interior at a scale of (b) 100 and (c) 10 mm. Reprinted with permission from ref 39. Copyright 2010 The Royal Society of Chemistry.

MOFs in membranes. Two categories of membranes can be distinguished: hybrid membranes and pure MOF membranes. Hybrid membranes are heterogeneous membranes in which a filler (in this instance, MOF powder or crystals) is embedded into a polymer matrix to improve the selectivity and/or permeability of pure polymeric membranes. These membranes will not be discussed here; details can be found elsewhere.[121,122] We will focus on pure MOF membranes, which consist of a dense, active MOF layer grown on a porous substrate, typically alumina or titania.

The first example of a dense and well-intergrown MOF membrane was reported by Liu et al.[46] The authors chose MOF-5 and prepared it as a layer on top of porous alumina by direct synthesis under solvothermal conditions. However, the performance of the membrane was notably poor; diffusion of the gases followed Knudsen diffusion, i.e., diffusion was proportional to the square root of the molar mass of the gas molecules. Such a behavior has also been observed for membranes with pinholes and microcracks that are not easy to detect by other methods, such as SEM. Nevertheless, the large size of MOF-5 pores (approximately 11 Å) renders a separation based on size criteria at room temperature impossible (the largest gas molecules have a kinetic diameter of approximately 5.5 Å).

Guo et al.[22] prepared a 60 μm thick membrane using copper net as a support. The MOF, HKUST-1, also contains large pores (9 Å × 9 Å) but exhibits a high selectivity for H_2 relative to N_2, CH_4, and CO_2, together with high permeation fluxes. The authors suggested that H_2 is much smaller than the other molecules, is not adsorbed into the network, and thus diffuses faster. Surprisingly, membranes featuring the same MOF but supported on alumina ceramic showed no selectivity for H_2.[31,38] Hu et al.[80] reported the first example of liquid separation with MIL-53 membranes. The large pores of MIL-53 (7.3 Å × 7.7 Å) prevent any gas separation above the Knudsen factor but could be useful for dehydration of water−solvent mixtures by pervaporation. A very good selectivity for water was observed when water−ethyl acetate mixtures were passed through the membranes at 60 °C: the feed contained only 7% water, whereas the permeate contained 99%. In addition, the membrane exhibited good stability after 200 h of operation.

Scheme 1. Reaction Conditions for Oxidation of Tetralin

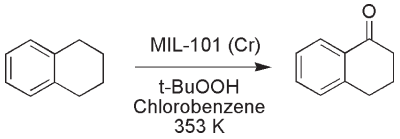

These few examples show that the choice of a MOF for membrane applications is of high importance. For instance, permeances in 1D pore systems may be greatly reduced by misoriented grains (from the seed layer or from the film itself) and intergrain boundaries.[82] Therefore, 3D pore systems should be preferred over 1D or 2D systems. In addition, the pore size should be taken into account. Indeed, molecular sieving is a straightforward and efficient way to probe the quality of a membrane, although it is not applicable for large-pore MOFs. Thus, Knudsen separation factors may be observed even for high-quality membranes that feature large pores and no specific interactions with gas molecules. Measurement of the permeances with increasing applied pressure can nevertheless suggest an absence of macroscopic defects if the values of the permeances remain constant.[45,46,80] In addition to the proper choice of MOFs with an adapted pore size, other approaches, such as pore functionalization, can also be used to introduce selectivity. Modification of only the external surface of a film by postsynthetic functionalization to reduce the accessible diameter of the pores is possible, as is postsynthetic modification of the whole framework and introduction of selective groups. Use of functional linkers is an additional possibility to induce selectivity and/or reduce the size of the pores. To the best of our knowledge, only the last two approaches have been reported.[63,71]

Several examples of MOF membranes for molecular-sieving membranes have been reported by Caro and co-workers. These membranes are based on the use of MOFs with small pores that form a 3D network. These MOFs belong to the zeolitic imidazolate framework (ZIF) family. ZIFs consist of transition metals (Zn, Co) and imidazolate linkers that form 3D tetrahedral frameworks and frequently resemble zeolite topologies. Some of them have exceptional thermal and chemical stabilities. ZIF-7, ZIF-8, ZIF-22, and ZIF-90 have been successfully applied as films on porous alumina and titania substrates.[51,57,58,60,62] The layers were grown in solvothermal solutions, often after substrate treatment or seeding to obtain dense and well-intergrown MOF films (see Figure 29). The films typically exhibit a thickness of 10−30 μm.

In this section, we will discuss in greater detail the membrane featuring ZIF-90.[62] ZIF-90 is built from Zn^{2+} ions and uses imidazolate-2-carboxyaldehyde (ICA) as the linker. It exhibits high thermal stability and a pore opening of approximately 3.5 Å. Therefore, a ZIF-90 membrane is expected to be able to separate hydrogen (kinetic diameter of approximately 2.9 Å) from larger gas molecules, such as CH_4. Prior to the permeation measurements, the membrane required an activation step to remove the solvent molecules that occluded during synthesis. This step was performed in situ in the permeation cell by supplying an equimolar mixture of H_2 and CH_4 while increasing the temperature. Interestingly, the permeance of H_2 increased up to a maximum value at 200 °C, whereas the permeance of CH_4 remained nearly constant. This corresponds to the molecular sieving effect: the methane molecules are too large. A separation factor of 15.2 was achieved for a H_2/CH_4 mixture at 200 °C (see Figure 30). The small permeance observed for large molecules

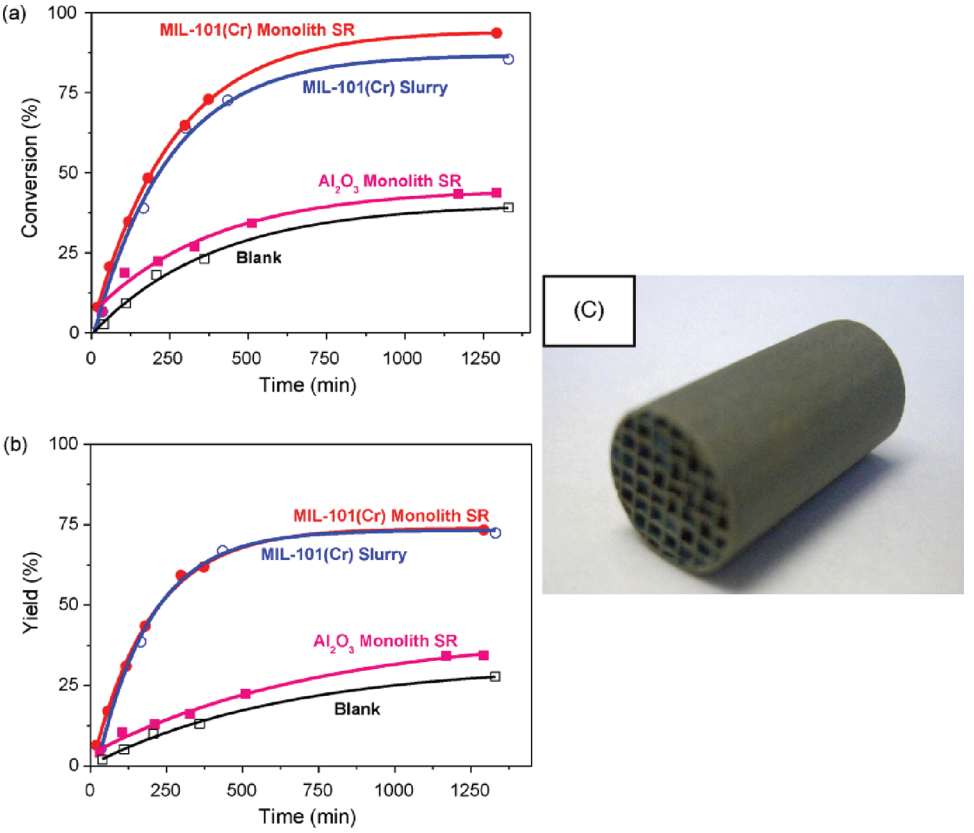

Figure 35. (a) Tetralin conversion versus time. (b) Tetralone yield with time. Comparison of the performance of MIL-101(Cr) in powder form (○) and coated on monolith (●) and of the monolith support itself (■). Blank experiment without catalyst (□). Reaction conditions: 8 mmol of tetralin, 16 mmol of *t*-BuOOH, 5 mL of chlorobenzene, T = 353 K, mcat = 50 mg. (c) Optical photograph of a coated monolith. Reprinted with permission from ref 88. Copyright 2011 Elsevier.

that are not expected to fit into the pores was attributed to the lattice flexibility of the MOF. The ZIF-90 membrane can separate H_2 from H_2/CH_4 mixtures at temperatures between 25 and 225 °C; the selectivity factor increases from 7 to 16.4 with increasing temperature. Interestingly, the membrane performances were stable even when water vapor was mixed into the feed stream, which means that the membrane exhibits high hydrothermal stability and is applicable for H_2 separation/purification at high temperature.

A further improvement of the membrane separation power has been achieved by covalent postfunctionalization.[63] Indeed, because the linker of ZIF-90 bears aldehyde groups, reactions such as imine condensation with amines are possible. The authors used ethanolamine to test the concept. An as-synthesized membrane was refluxed with ethanolamine in a methanol solution at 60 °C. X-ray diffraction indicated no changes in the crystallinity of the membrane. The covalent postsynthetic functionalization is thought to have two effects: a slight reduction of the size of the pores and a reduction of the diffusion through intercrystalline defects. As a result, the H_2/CO_2 selectivity at room temperature increased from 7.2 to 15.7.

As previously discussed, use of functional linkers is another way to introduce gas selectivity in a MOF membrane. We recently prepared membranes by the stepwise deposition of reactants with either $[Cu_2(ndc)_2(dabco)]$ or $[Cu_2(BME\text{-}bdc)_2(dabco)]$.[71] $[Cu_2(ndc)_2(dabco)]$ is a large-pore MOF in which no specific interactions occur between the framework and gaseous molecules. As a result, Knudsen separation factors were obtained. BME-bdc consists of a benzene ring with two long ether side groups ($-O(CH_2)_2OCH_3$) and is known to induce selectivity toward CO_2 in the isoreticular $[Zn_2(BME\text{-}bdc)_2(dabco)]$.[123] The membrane featuring $[Cu_2(BME\text{-}bdc)_2(dabco)]$ also displayed selectivity toward CO_2, particularly when compared to CH_4. Equimolar mixtures of CO_2/CH_4 were separated with a selectivity factor of 4.5, which is well above the corresponding Knudsen coefficient (0.6). Because of the dynamic behavior of the ether side groups, it is not possible to evaluate the size of the pores from the crystal structure, although we can approximate their size as between 3.5 and 4 Å. Therefore, the separation cannot be attributed solely to molecular sieving but rather to preferential interactions between CO_2 and the framework.

4.3.2. Separation by Chromatography. The large diversity in the structures and pore sizes, adsorption affinities, and selective penetrations makes MOFs attractive as chromatographic separation media. A few groups have already reported the separation of xylenes[124] as well as branched and linear alkanes[125] using chromatography columns filled with MIL-101(Cr) and ZIF-8, respectively. However, it would be interesting to directly grow the MOF as a film from the inner surface of the column, particularly in a capillary being used in gas chromatography. The most widely adapted method for that purpose appears to be stepwise deposition, because the concentration of reactants along the capillary as well as from cycle to cycle remains constant; the surface can thus be uniformly saturated with either the metal or the linker at each step.

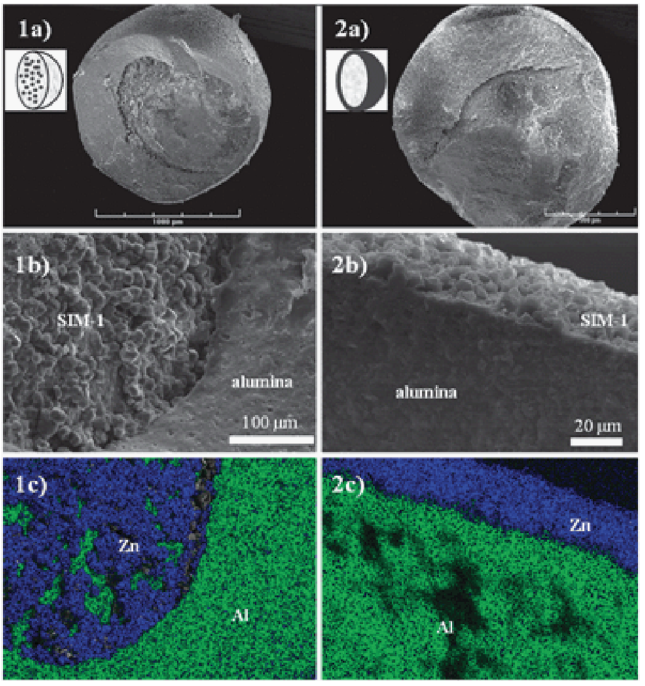

Figure 36. SIM-1 supported on γ- (1) and α-alumina beads (2). (a) SEM image of the bead; view of the cross-section. (b) SEM image and (c) EDXS mapping of the core (1) or surface (2). Color code: blue, Zn; green, Al. Reprinted with permission from ref 65. Copyright 2010 The Royal Society of Chemistry.

A demonstration of this concept was recently reported by Mertens and co-workers,[47] who coated a narrow gas-chromatographic fused-silica capillary (length 10 m, clear diameter 0.53 mm). They first functionalized the inner surface with a SAM prepared from $HOOC(CH_2)_9SiCl_3$ and then grew MOF-5 on it by alternately using basic zinc acetate in DMF as the precursor and terephthalic acid in DMF as the linker solution. These components were alternately pumped through the capillary at room temperature via an automated apparatus (see Figure 31). Excess solvent was removed by a stream of argon instead of by rinsing with the solvent. This coating procedure was inspired by the controlled SBU approach for IRMOFs.[95] As expected, the grown MOF material uniformly covered the capillary across its entire length. The 80 cycles led to a coating thickness of approximately 1 μm. This significantly large thickness is at least partly explained by the surface storage effect, i.e., insufficient desolvation of the already formed MOF material.

The MOF-5-coated column was tested and compared to a commercial PLOT column for analysis of natural gas. In both columns, the main components of natural gas (C1−C4 alkanes) were clearly separated. However, the MOF-coated column separated the components faster with otherwise comparable performances (see Figure 32). To further test the possibility of such a GC capillary, additional components (from commercial butane gas) were added to the feed. Thus, a total of nine components had to be separated. The results plotted in Figure 32b clearly show a good separation with the signal returning to baseline between two neighboring peaks. Such good results obtained at the start of the development of MOF-based columns, without any optimization of the MOF toward this specific separation problem, are promising for development of future applications.

4.4. Catalysis

Adaptation of MOFs as heterogeneous catalysts is highly desirable, and numerous studies have shown that activity and selectivity can be obtained for a large number of reactions.[126] However, examples of MOF coatings used in catalysis are very rare.

Early studies on MOF-5 polycrystalline films showed that it is possible to load the pores of a film with an organometallic precursor, e.g., $[(\eta^5\text{-}C_5H_5)Pd(\eta^3\text{-}C_3H_5)]$, by gas-phase loading after preliminary activation.[42,43] The film turned deep red upon loading with the red compound. Subsequent reduction of the precursor by H_2 or photolysis by UV light led to palladium particles embedded into the film, as shown by its black color (see Figure 33). X-ray analysis showed that the framework was still intact and that 1.4 nm Pd particles are formed. The loading of MOF-5 with Pd particles was studied in detail on bulk samples, which proved to be moderately active catalysts for hydrogenation of cyclooctene.[127] Processed as thin films, such metal@MOF materials could open pathways to catalytically active electrodes or sensors.

For applications in catalytic reactors, however, it is advantageous to shape the MOF on macroscopic supports, such as monoliths. A few pioneering works report the fabrication of composites MOF@macroporous supports. Schwab et al.[40] have grown HKUST-1 crystals inside the macropores of polymeric foam supports called polyHIPES by three successive steps of growth in a mother solution. A maximum loading of 62.3% was obtained, but the density of the incorporated crystals was nonetheless low. O'Neill et al.[39] prepared HKUST-1 composites beads where the beads consisted of macroporous polyacrylamide (PAM) or silica-PAM (see Figure 34). Direct synthesis under solvothermal conditions or in an aged mother solution at room temperature were used; however, in the latter case, MOF growth occurred only if the beads had been previously immersed in copper acetate aqueous solutions. This effect was attributed to the low and ill-controlled number of functional groups at the surface. Control of the density of the MOF crystals, and thus the total BET surface area of the composites, could be achieved by simply tuning the concentration of reactants during solvothermal synthesis.

The first example of catalysis with MOF films has recently been reported by Ramos-Fernandez et al.[88] They used cylindrical cordierite monolithic substrates and coated them with MIL-101 (Cr) using a seeded growth process: the monoliths were immersed in a NaOH solution and then in a mixture of α-alumina and MIL-101 (Cr) particles (respective sizes of 100 and 150 nm) and calcined at 400 °C. This procedure simulates application of a washcoat, which greatly improves the surface area of the monolith. The seeded monoliths were then subjected to a secondary growth step in a rotating autoclave, and homogeneous coatings were obtained. The coated monoliths were subsequently used as catalysts for oxidation of tetralin at 353 K (see Scheme 1).

The results are summarized in Figure 35. For purposes of comparison, MIL-101(Cr) was used as a powder in a slurry reactor, an alumina coated monolith was also tested, and a blank reaction without solid was performed. The results indeed showed a catalytic effect of MIL-101 (Cr). Interestingly, the coated monolith performed slightly better than did the slurry reactor. Activity and selectivity were mostly retained for five runs after regeneration, whereas in the case of the slurry reactor 20% of the powder was lost during filtration of the reactive mixture.

Aguado et al.[65] coated α- and γ-alumina beads with a MOF belonging to the ZIF family, SIM-1, by direct synthesis in solvothermal solution at 85 °C for 48 h. In both cases, loading

was estimated at 10% and the presence of the MOF was confirmed by XRD and EDXS (see Figure 36). To explain the high affinity of the MOF for the substrate, the authors performed IR spectroscopy and found ester bonds, which suggests that the aldehyde groups of the linker were bound to Al−OH surface groups. To test the catalytic activity of the beads, reduction of acetophenone to phenylethanol by transfer hydrogenation was performed in isopropanol. The supported MOF exhibited an activity similar to that of the MOF alone; it also exhibited good reusability and was easily recovered.

5. CONCLUSION

The field of metal−organic framework films bears a huge potential for both fundamental understanding and practical applications. As a consequence, the field has been increasingly growing over the past few years and a huge number of contributions have come out since the first review was published.[15] Many new fabrication concepts have emerged; clear improvements have been made in the control of key parameters, such as microstructure and orientation. Understanding the growth mechanisms for SURMOFs, as well as for polycrystalline films, is steadily increasing.

New ideas and concepts for films often come from the bulk MOF community. Indeed, in-depth studies of new properties, as well as fine structure tuning, are easier to perform on powders or single crystals before being transferred to films. MOF-on-MOF heterostructures, postfunctionalization, loading, and catalysis are typical examples. Nevertheless, many concepts have not yet been applied to thin films despite undeniable interest in such applications. This category includes luminescent films (only one mechanism among those possible (see section 4.2.3) has been described), magnetic films, redox-active films, and proton- or electron-conducting films. Membranes that comprise proton-conducting MOF materials could, for example, be used in polymer electrolyte membrane-type fuel cells at elevated temperature (150 °C), whereas conventional fuel cells are limited by the water-dependent proton conduction in the polymer electrolyte.[128,129] Electrically conductive porous films would have numerous applications as electrodes. Redox-active films could be used as sensors or catalysts. Luminescent or magnetic films could also be used as sensors. Applied to SURMOF, the concept of multivariate MOFs recently introduced by Yaghi and co-workers[6] may lead to totally new properties, especially when combined with MOF-on-MOF-type architectures.

The MOF thin-film field, however, can also provide valuable input to the broader MOF community. The SBU-controlled approach is supported by evidence from SURMOF liquid-phase epitaxial deposition: HKUST-1 can grow only when $Cu(OAc)_2$ is used as the precursor. Insights on the nucleation mechanisms have been obtained from an in-situ AFM study during liquid-phase epitaxy. Diffusivity values were easily measured. New MOF structures, either noninterpenetrated versions of already existing MOFs or completely new ones, have been obtained. Certain application concepts, such as fabrication of composite membranes or porous multilayer assemblies (e.g., Bragg stacks), are possible only when MOFs are processed as thin films. Thus far, only membrane fabrication has been investigated; the optical properties of well-defined multilayered MOF thin films remain largely unexplored.

As indicated by perusing the body of literature dealing with applications of MOF films, mostly proofs of principle have been achieved. Truly functional devices or catalysts will certainly require several years or more to be developed. New problems will be faced, such as the scale-up and automation of deposition procedures. These procedures will certainly need to be modified; to date, electrochemical processes and stepwise deposition of reactants appear to be the most promising approaches. It also appears that only a small number of potential applications have been demonstrated among the large number of those that are possible. With this review, we hope to inspire the reader with new ideas and to stimulate the emergence of new concepts and applications in the field of MOF thin films.

AUTHOR INFORMATION

Corresponding Author

*E-mail: roland.fischer@rub.de.

BIOGRAPHIES

Angélique Bétard, born 1986, studied physics and chemistry at the Ecole Supérieure de Physique et Chimie Industrielles in Paris, where she obtained her engineer diploma in 2009. During the course of her studies, she worked 6 months as a research assistant at Kodak European Research (Cambridge, U.K.) and did internships at the Institut Curie and Ecole Supérieure de Chimie in Paris. In addition, she received her M.Sc. degree in Materials Science from Université Pierre et Marie Curie (Paris). Since 2009, she has been working as a Ph.D. student under the supervision of Prof. Roland A. Fischer at Ruhr-Universität Bochum with the support of a DAAD fellowship. Her research interests focus on MOF thin-film growth and characterization.

Roland A. Fischer studied chemistry at the Technische Universität München (TUM) and received his Dr. rer. nat. degree in

1989 under the guidance of Wolfgang A. Herrmann. After a postdoctoral collaboration with Herb D. Kaesz at the University of California, Los Angeles (UCLA), he returned to TUM in 1990, where he obtained his Habilitation in 1995. In 1996 he was appointed Associate Professor at the Ruprecht-Karls Universität in Heidelberg. In 1998 he moved to the Ruhr-Universität Bochum, where he took the chair in Inorganic Chemistry II. He was Dean of the Ruhr University Research School (2006−2009). His research interests focus on group 13/transition metal compounds, precursor chemistry for inorganic materials, chemical vapor deposition (CVD), thin films, nanoparticles, colloids, and the supramolecular host guest chemistry of porous coordination polymers (MOFs).

ACKNOWLEDGMENT

A.B. is grateful to the DAAD institution for a fellowship and thanks the Ruhr University Research School (http://www.research-school.rub.de) for additional support. R.A.F. is particularly grateful to the German Research Foundation (DFG) and the European Union for funding the research projects on MOF thin films (Priority Program 1362 of the DFG) and SURMOFs (sixth FP, NMP4-CT-2006-032109). The numerous stimulating discussions and ongoing fruitful collaboration with Christof Wöll and co-workers at the Karlsruhe Institute of Technology are also gratefully acknowledged.

LIST OF ACRONYMS

AFM: atomic force microscopy
bdc: 1,4-benzene dicarboxylate
4,4′-bipy: 4,4′-bipyridine
BME-bdc: 2,5-bis(2-methoxyethoxy)-1,4-benzene dicarboxylate
btc: benzene-1,3,5-tricarboxylate
CSA: controlled SBU approach
dabco: 1,4-diazabicyclo(2.2.2)octane
DEF: *N*,*N*-diethylformamide
DMF: *N*,*N*-dimethylformamide
F_4bdc: tetrafluoro-1,4-benzene dicarboxylate
GC: gas chromatography
H_2hfipbb: 4,4′-(hexafluoroisopropylidene)-bis(benzoic acid)
HKUST: Hong-Kong University of Science and Technology
MIL: Material of Institut Lavoisier
MOF: metal−organic framework
NAFS: nanofilm on a solid surface
ndc: 1,4-naphtalene dicarboxylate
pyz: pyrazine
pzdc: pyrazine-2,3-dicarboxylate
QCM: quartz crystal microbalance
SBU: secondary building unit
SAM: self-assembled monolayer
SEM: scanning electron microscopy
TGA: thermogravimetric analysis
XPS: X-ray photoelectron spectroscopy
XRD: X-ray diffraction
ZIF: zeolitic imidazolate framework

REFERENCES

(1) Li, H.; Eddaoudi, M.; O'Keeffe, M.; Yaghi, O. M. *Nature* **1999**, *402*, 276.
(2) Kitagawa, S.; Kitaura, R.; Noro, S. *Angew. Chem., Int. Ed.* **2004**, *43*, 2334.
(3) Eddaoudi, M.; Kim, J.; Rosi, N. L.; Vodak, D.; Wachter, J.; O'Keeffe, M.; Yaghi, O. M. *Science* **2002**, *295*, 469.
(4) Wang, Z.; Cohen, S. M. *Chem. Soc. Rev.* **2009**, *38*, 1315.
(5) Yamada, T.; Kitagawa, H. *J. Am. Chem. Soc.* **2009**, *131*, 6312.
(6) Deng, H.; Doonan, C. J.; Furukawa, H.; Ferreira, R. B.; Towne, J.; Knobler, C. B.; Wang, B.; Yaghi, O. M. *Science* **2010**, *327*, 846.
(7) Furukawa, S.; Hirai, K.; Nakagawa, K.; Takashima, Y.; Matsuda, R.; Tsuruoka, T.; Kondo, M.; Haruki, R.; Tanaka, D.; Sakamoto, H.; Shimomura, S.; Sakata, O.; Kitagawa, S. *Angew. Chem., Int. Ed.* **2009**, *48*, 1766.
(8) Koh, K.; Wong-Foy, A. G.; Matzger, A. J. *Chem. Commun.* **2009**, 6162.
(9) Allendorf, M. D.; Bétard, A.; Fischer, R. A. In *Metal-Organic Frameworks: Applications from Catalysis to Gas Storage*; Farrusseng, D., Ed.; Wiley-VCH: Weinheim, 2011.
(10) Gascon, J.; Kapteijn, F. *Angew. Chem., Int. Ed.* **2010**, *49*, 1530.
(11) Lew, C. M.; Cai, R.; Yan, Y. *Acc. Chem. Res.* **2010**, *43*, 210.
(12) Snyder, M. A.; Tsapatsis, M. *Angew. Chem., Int. Ed.* **2007**, *46*, 7560.
(13) Culp, J. T.; Park, J.-H.; Benitez, I. O.; Huh, Y.-D.; Meisel, M. W.; Talham, D. R. *Chem. Mater.* **2003**, *15*, 343.
(14) Culp, J. T.; Park, J.-H.; Frye, F.; Huh, Y.-D.; Meisel, M. W.; Talham, D. R. *Coord. Chem. Rev.* **2005**, *2005*, 2642.
(15) Zacher, D.; Shekhah, O.; Wöll, C.; Fischer, R. A. *Chem. Soc. Rev.* **2009**, *38*, 1418.
(16) Shekhah, O.; Liu, J.; Fischer, R. A.; Wöll, C. *Chem. Soc. Rev.* **2011**, *40*, 1081.
(17) Zacher, D.; Schmid, R.; Wöll, C.; Fischer, R. A. *Angew. Chem., Int. Ed.* **2011**, *50*, 176.
(18) Zacher, D.; Baunemann, A.; Hermes, S.; Fischer, R. A. *J. Mater. Chem* **2007**, *17*, 2785.
(19) Gascon, J.; Aguado, S.; Kapteijn, F. *Microporous Mesoporous Mater.* **2008**, *113*, 132.
(20) Biemmi, E.; Scherb, C.; Bein, T. *J. Am. Chem. Soc.* **2007**, *129*, 8054.
(21) Biemmi, E.; Darga, A.; Stock, N.; Bein, T. *Microporous Mesoporous Mater.* **2008**, *114*, 380.
(22) Guo, H.; Zhu, G.; Hewitt, I. J.; Qiu, S. *J. Am. Chem. Soc.* **2009**, *131*, 1646.
(23) Ameloot, R.; Stappers, L.; Fransaer, J.; Alaerts, L.; Sels, B. F.; De Vos, D. E. *Chem. Mater.* **2009**, *21*, 2580.
(24) Ameloot, R.; Pandey, L.; Van der Auweraer, M.; Alaerts, L.; Sels, B. F.; De Vos, D. E. *Chem. Commun.* **2010**, *45*, 3735.
(25) Shekhah, O.; Wang, H.; Kowarik, S.; Schreiber, F.; Paulus, M.; Tolan, M.; Sternemann, C.; Evers, F.; Zacher, D.; Fischer, R. A.; Wöll, C. *J. Am. Chem. Soc.* **2007**, *129*, 15118.
(26) Shekhah, O.; Wang, H.; Zacher, D.; Fischer, R. A.; Wöll, C. *Angew. Chem., Int. Ed.* **2009**, *48*, 5038.
(27) Zybaylo, O.; Shekhah, O.; Wang, H.; Tafipolsky, M.; Schmid, R.; Johannsmann, D.; Wöll, C. *Phys. Chem. Chem. Phys.* **2010**, *12*, 8092.
(28) Allendorf, M. D.; Houk, R. J. T.; Andruszkiewicz, L.; Talin, A. A.; Pikarsky, J.; Choudhury, A.; Gall, K. A.; Hesketh, P. J. *J. Am. Chem. Soc.* **2008**, *130*, 14404.
(29) Kreno, L. E.; Hupp, J. T.; Van Duyne, R. P. *Anal. Chem.* **2010**, *82*, 8042.
(30) Schoedel, A.; Scherb, C.; Bein, T. *Angew. Chem., Int. Ed.* **2010**, *49*, 7225.
(31) Varela-Guerrero, V.; Yoo, Y.; McCarthy, M. C.; Jeong, H.-K. *J. Mater. Chem* **2010**, *20*, 3938.
(32) Küsgens, P.; Siegle, S.; Kaskel, S. *Adv. Eng. Mater.* **2009**, *11*, 93.
(33) Ameloot, R.; Gobechiya, E.; Uji-i, H.; Martens, J. A.; Hofkens, J.; Alaerts, L.; Sels, B. F.; De Vos, D. E. *Adv. Mater.* **2010**, *22*, 2685.
(34) Carbonell, C.; Imaz, I.; Maspoch, D. *J. Am. Chem. Soc.* **2011**, *133*, 2144.
(35) Kayaert, S.; Bajpe, S.; Masschaele, K.; Breynaert, E.; Kirschhock, C. E. A.; Martens, J. A. *Thin Solid Films* **2011**, *519*, 5347.
(36) Liu, J.; Sun, F.; Zhang, F.; Wang, Z.; Zhang, R.; Wang, C.; Qiu, S. *J. Mater. Chem* **2011**, *21*, 3775.

(37) Meilikhov, M.; Yusenko, K.; Schollmeyer, E.; Mayer, C.; Buschmann, H.-J.; Fischer, R. A. *Dalton Trans.* **2011**, *40*, 4838.
(38) Nan, J.; Dong, X.; Wang, W.; Jin, W.; Xu, N. *Langmuir* **2011**, *27*, 4309.
(39) O'Neill, L. D.; Zhang, H.; Bradshaw, D. *J. Mater. Chem* **2010**, *20*, 5720.
(40) Schwab, M. G.; Senkovska, I.; Rose, M.; Koch, M.; Pahnke, J.; Jonschker, G.; Kaskel, S. *Adv. Eng. Mater.* **2008**, *10*, 1151.
(41) Zhuang, J.-L.; Ceglarek, D.; Pethuraj, S.; Terfort, A. *Adv. Funct. Mater.* **2011**, *21*, 1442.
(42) Hermes, S.; Schröder, F.; Chelmowski, R.; Wöll, C.; Fischer, R. A. *J. Am. Chem. Soc.* **2005**, *127*, 13744.
(43) Hermes, S.; Zacher, D.; Baunemann, A.; Wöll, C.; Fischer, R. A. *Chem. Mater.* **2007**, *19*, 2168.
(44) Yoo, Y.; Jeong, H.-K. *Chem. Commun.* **2008**, 2441.
(45) Yoo, Y.; Lai, Z.; Jeong, H.-K. *Microporous Mesoporous Mater.* **2009**, *123*, 100.
(46) Liu, Y.; Ng, Z.; Khan, E. A.; Jeong, H.-K.; Ching, C.-b.; Lai, Z. *Microporous Mesoporous Mater.* **2009**, *118*, 296.
(47) Münch, A. S.; Seidel, J.; Obst, A.; Weber, E.; Mertens, F. O. R. L. *Chem.—Eur. J.* **2011**, DOI: 10.1002/chem.201100642.
(48) Falcaro, P.; Hill, A. J.; Nairn, K. M.; Jasieniak, J.; Mardel, J. I.; Bastow, T. J.; Mayo, S. C.; Gimona, M.; Gomez, D.; Whitfield, H. J.; Riccò, R.; Patelli, A.; Marmiroli, B.; Amenitsch, H.; Colson, T.; Villanova, L.; Buso, D. *Nat. Commun.* **2011**, *2*, 237.
(49) Lu, G.; Hupp, J. T. *J. Am. Chem. Soc.* **2010**, *132*, 7832.
(50) Demessence, A.; Boissière, C.; Grosso, D.; Horcajada, P.; Serre, C.; Férey, G.; Soler-Illia, G. J. A. A.; Sanchez, C. *J. Mater. Chem* **2010**, *20*, 7676.
(51) Bux, H.; Liang, F.; Li, Y.; Cravillon, J.; Wiebcke, M.; Caro, J. *J. Am. Chem. Soc.* **2009**, *131*, 16000.
(52) Bux, H.; Chmelik, C.; Krishna, R.; Caro, J. *J. Membr. Sci.* **2010**, *369*, 284.
(53) Bux, H.; Feldhoff, A.; Cravillon, J.; Wiebcke, M.; Li, Y.-s.; Caro, J. *Chem. Mater.* **2011**, *23*, 2262.
(54) Venna, S. R.; Carreon, M. A. *J. Am. Chem. Soc.* **2009**, *132*, 76.
(55) McCarthy, M. C.; Varela-Guerrero, V.; Barnett, G. V.; Jeong, H.-K. *Langmuir* **2010**, *26*, 14636.
(56) Yao, J.; Dong, D.; Li, D.; He, L.; Xu, G.; Wang, H. *Chem. Commun.* **2011**, *47*, 2559.
(57) Li, Y.-S.; Liang, F.-Y.; Bux, H.; Feldhoff, A.; Yang, W.-S.; Caro, J. *Angew. Chem., Int. Ed.* **2010**, *49*, 548.
(58) Li, Y.-S.; Bux, H.; Feldhoff, A.; Li, G.-L.; Yang, W.-S.; Caro, J. *Adv. Mater.* **2010**, *22*, 3322.
(59) Li, Y.; Liang, F.; Bux, H.; Yang, W.; Caro, J. *J. Membr. Sci.* **2010**, *354*, 48.
(60) Huang, A.; Bux, H.; Steinbach, F.; Caro, J. *Angew. Chem., Int. Ed.* **2010**, *49*, 4958.
(61) Liu, Y.; Hu, E.; Khan, E. A.; Lai, Z. *J. Membr. Sci.* **2010**, *353*, 36.
(62) Huang, A.; Dou, W.; Caro, J. *J. Am. Chem. Soc.* **2010**, *132*, 15562.
(63) Huang, A.; Caro, J. *Angew. Chem., Int. Ed.* **2011**, *50*, 4979.
(64) Kubo, M.; Chaikittisilp, W.; Okubo, T. *Chem. Mater.* **2008**, *20*, 2887.
(65) Aguado, S.; Canivet, J.; Farrusseng, D. *Chem. Commun.* **2010**, *46*, 7999.
(66) Aguado, S.; Nicolas, C.-H.; Moizan-Baslé, V.; Nieto, C.; Amrouche, H.; Bats, N.; Audebrand, N.; Farrusseng, D. *New J. Chem.* **2011**, *35*, 41.
(67) Makiura, R.; Motoyama, S.; Umemura, Y.; Yamanaka, H.; Sakata, O.; Kitagawa, H. *Nat. Mater.* **2010**, *9*, 565.
(68) Motoyama, S.; Makiura, R.; Sakata, O.; Kitagawa, H. *J. Am. Chem. Soc.* **2011**, *133*, 5640.
(69) Shekhah, O.; Wang, H.; Paradinas, M.; Ocal, C.; Schüpbach, B.; Terfort, A.; Zacher, D.; Fischer, R. A.; Wöll, C. *Nat. Mater.* **2009***8*, 481.
(70) Yusenko, K.; Meilikhov, M.; Zacher, D.; Wieland, F.; Sternemann, C.; Stammer, X.; Ladnorg, T.; Wöll, C.; Fischer, R. A. *CrystEngComm* **2010**, *12*, 2086.
(71) Bétard, A.; Bux, H.; Henke, S.; Zacher, D.; Caro, J.; Fischer, R. A. *Microporous Mesoporous Mater.* DOI: 10.1016/j.micromeso.2011.09.006.
(72) Zacher, D.; Yusenko, K.; Bétard, A.; Henke, S.; Molon, M.; Ladnorg, T.; Shekhah, O.; Schüpbach, B.; Arcos, T. D. L.; Krasnopolski, M.; Meilikhov, M.; Winter, J.; Terfort, A.; Wöll, C.; Fischer, R. A. *Chem.—Eur. J.* **2011**, *17*, 1448.
(73) Shekhah, O.; Hirai, K.; Wang, H.; Uehara, H.; Kondo, M.; Diring, S.; Zacher, D.; Fischer, R. A.; Sakata, O.; Kitagawa, S.; Furukawa, S.; Wöll, C. *Dalton Trans.* **2011**, *40*, 4954.
(74) Liu, B.; Ma, M.; Zacher, D.; Bétard, A.; Yusenko, K.; Metzler-Nolte, N.; Wöll, C.; Fischer, R. A. *J. Am. Chem. Soc.* **2011**, *133*, 1734.
(75) Bétard, A.; Zacher, D.; Fischer, R. A. *CrystEngComm* **2010**, *12*, 3768.
(76) Centrone, A.; Yang, Y.; Speakman, S.; Bromberg, L.; Rutledge, G. C.; Hatton, T. A. *J. Am. Chem. Soc.* **2010**, *132*, 15687.
(77) Yoo, Y.; Jeong, H.-K. *Cryst. Growth Des.* **2010**, *10*, 1283.
(78) Yoo, Y.; Varela-Guerrero, V.; Jeong, H.-K. *Langmuir* **2011**, *27*, 2652.
(79) Arnold, M.; Kortunov, P.; Jones, D. J.; Nedellec, Y.; Kärger, J.; Caro, J. *Eur. J. Inorg. Chem.* **2007**, 60.
(80) Hu, Y.; Dong, X.; Nan, J.; Jin, W.; Ren, X.; Xu, N.; Lee, Y. M. *Chem. Commun.* **2010**, *47*, 737.
(81) Hinterholzinger, F.; Scherb, C.; Ahnfeldt, T.; Stock, N.; Bein, T. *Phys. Chem. Chem. Phys.* **2010**, *12*, 4514.
(82) Ranjan, R.; Tsapatsis, M. *Chem. Mater.* **2009**, *21*, 4920.
(83) Zou, X.; Zhu, G.; Zhang, F.; Guo, M.; Qiu, S. *CrystEngComm* **2010**, *12*, 352.
(84) Scherb, C.; Koehn, R.; Bein, T. *J. Mater. Chem* **2010**, *20*, 3046.
(85) Scherb, C.; Schödel, A.; Bein, T. *Angew. Chem., Int. Ed.* **2008**, *47*, 5777.
(86) Horcajada, P.; Serre, C.; Grosso, D.; Boissière, C.; Perruchas, S.; Sanchez, C.; Férey, G. *Adv. Mater.* **2009**, *21*, 1931.
(87) Demessence, A.; Horcajada, P.; Serre, C.; Boissière, C.; Grosso, D.; Sanchez, C.; Férey, G. *Chem. Commun.* **2009**, *101*, 7149.
(88) Ramos-Fernandez, E. V.; Garcia-Domingos, M.; Juan-Alcañiz, J.; Gascon, J.; Kapteijn, F. *Appl. Catal. A: Gen.* **2011**, *391*, 261.
(89) Zou, X.; Zhu, G.; Hewitt, I. J.; Sun, F.; Qiu, S. *Dalton Trans.* **2009**, 3009.
(90) Decher, G. *Science* **1997**, *277*, 1232.
(91) Bell, C. M.; Arendt, M. F.; Gomez, L.; Schmehl, R. H.; Mallouk, T. E. *J. Am. Chem. Soc.* **1994**, *116*, 8374.
(92) Cobo, S.; Molnár, G.; Real, J. A.; Bousseksou, A. *Angew. Chem., Int. Ed.* **2006**, *45*, 5786.
(93) Molnár, G.; Cobo, S.; Real, J. A.; Carcenac, F.; Daran, E.; Vieu, C.; Bousseksou, A. *Adv. Mater.* **2007**, *19*, 2163–2167.
(94) Munuera, C.; Shekhah, O.; Wang, H.; Wöll, C.; Ocal, C. *Phys. Chem. Chem. Phys.* **2008**, *10*, 7257.
(95) Hausdorf, S.; Baitalow, F.; Böhle, T.; Rafaja, D.; Mertens, F. O. R. L. *J. Am. Chem. Soc.* **2010**, *132*, 10978.
(96) Kitaura, R.; Seki, K.; Akiyama, G.; Kitagawa, S. *Angew. Chem., Int. Ed.* **2003**, *42*, 428.
(97) Klinowski, J.; Almeida Paz, F. A.; Silva, P.; Rocha, J. *Dalton Trans.* **2011**, *40*, 321.
(98) Yaghi, O. M.; Li, G.; Li, H. *Chem. Mater.* **1997**, *9*, 1074.
(99) Spokoyny, A. M.; Kim, D.; Sumrein, A.; Mirkin, C. A. *Chem. Soc. Rev.* **2009**, *38*, 1218.
(100) Tsuruoka, T.; Furukawa, S.; Takashima, Y.; Yoshida, K.; Isoda, S.; Kitagawa, S. *Angew. Chem., Int. Ed.* **2009**, *48*, 4739.
(101) Mueller, U.; Schubert, M.; Teich, F.; Puetter, H.; Schierle-Arndt, K.; Pastre, J. *J. Mater. Chem* **2006**, *16*, 626.
(102) Makiura, R.; Kitagawa, H. *Eur. J. Inorg. Chem.* **2010**, 3715.
(103) Taniguchia, T.; Watanebeb, T.; Ichinoheb, S.; Yoshimuraa, M.; Katsumataa, K.-I.; Okadaa, K.; Matsushita, N. *Nanoscale* **2010**, *2*, 1426.
(104) Sauerbrey, G. *Z. Phys.* **1959**, *155*, 206.
(105) Li, J.-R.; Kuppler, R. J.; Zhou, H.-C. *Chem. Soc. Rev.* **2009**, *38*, 1477.

(106) Tzoulaki, D.; Heinke, L.; Lim, H.; Li, J.; Olson, D.; Caro, J.; Krishna, R.; Chmelik, C.; Kärger, J. *Angew. Chem., Int. Ed.* **2009**, *48*, 3525.
(107) Schneemann, A.; A. Bétard, Zacher, D.; Fischer, R.A. Unpublished results
(108) Gadzikwa, T.; Lu, G.; Stern, C. L.; Wilson, S. R.; Hupp, J. T.; Nguyen, S. T. *Chem. Commun.* **2008**, 5493.
(109) Kondo, M.; Furukawa, S.; Hirai, K.; Kitagawa, S. *Angew. Chem., Int. Ed.* **2010**, *49*, 5327.
(110) Gassensmith, J. J.; Erne, P. M.; Paxton, W. F.; Valente, C.; Stoddart, J. F. *Langmuir* **2011**, *24*, 1341.
(111) Ferreira, G. N. M.; Da-Silva, A.-C.; Tomé, B. *Trends Biotechnol.* **2009**, *27*, 689.
(112) Boissiere, C.; Grosso, D.; Lepoutre, S.; Nicole, L.; Bruneau, A. B.; Sanchez, C. *Langmuir* **2005**, *21*, 12362.
(113) Takashima, Y.; Martínez, V. M.; Furukawa, S.; Kondo, M.; Shimomura, S.; Uehara, H.; Nakahama, M.; Sugimoto, K.; Kitagawa, S. *Nat. Commun.* **2011**, *2*, 168.
(114) Lan, A.; Li, K.; Wu, H.; Olson, D. H.; Emge, T. J.; Ki, W.; Hong, M.; Li, J. *Angew. Chem., Int. Ed.* **2009**, *48*, 2334.
(115) Harbuzaru, B. V.; Corma, A.; Rey, F.; Atienzar, P.; Jordá, J. L.; García, H.; Ananias, D.; Carlos, L. D.; Rocha, J. *Angew. Chem., Int. Ed.* **2008**, *120*, 1096.
(116) Luo, F.; Batten, S. R. *Dalton Trans.* **2010**, *39*, 4485.
(117) Doty, F. P.; Bauer, C. A.; Skulan, A. J.; Grant, P. G.; Allendorf, M. D. *Adv. Mater.* **2009**, *21*, 95.
(118) Achmann, S.; Hagen, G.; Kita, J.; Malkowsky, I. M.; Kiener, C.; Moos, R. *Sensors* **2009**, *9*, 1574.
(119) Southon, P. D.; Liu, L.; Fellows, E. A.; Price, D. J.; Halder, G. J.; Chapman, K. W.; Moubaraki, B.; Murray, K. S.; Létard, J.-F.; Kepert, C. J. *J. Am. Chem. Soc.* **2009**, *131*, 10998.
(120) Maspoch, D.; Ruiz-Molina, D.; Wurst, K.; Domingo, N.; Cavallini, M.; Biscarini, F.; Tejada, J.; Rovira, C.; Veciana, J. *Nat. Mater.* **2003**, *2*, 190.
(121) Keskin, S.; van Heest, T. M.; Sholl, D. S. *ChemSusChem* **2010**, *3*, 879.
(122) Basu, S.; Cano-Odena, A.; Vankelecom, I. F. J. *J. Membr. Sci.* **2010**, *362*, 478.
(123) Henke, S.; Schmid, R.; Grunwaldt, J.-D.; Fischer, R. A. *Chem.—Eur. J.* **2010**, *16*, 14296.
(124) Gu, Z.-Y.; Yan, X.-P. *Angew. Chem., Int. Ed.* **2010**, *49*, 1477.
(125) Chang, N.; Gu, Z.-Y.; Yan, X.-P. *J. Am. Chem. Soc.* **2010**, *132*, 13645.
(126) Corma, A.; García, H.; Llabrés i Xamena, F. X. *Chem. Rev.* **2010**, *110*, 4606.
(127) Hermes, S.; Schröter, M.-K.; Schmid, R.; Khodeir, L.; Muhler, M.; Tissler, A.; Fischer, R. W.; Fischer, R. A. *Angew. Chem., Int. Ed.* **2005**, *44*, 6237.
(128) Bureekaew, S.; Horike, S.; Higuchi, M.; Mizuno, M.; Kawamura, T.; Tanaka, D.; Yanai, N.; Kitagawa, S. *Nat. Mater.* **2009**, *8*, 831.
(129) Hurd, J. A.; Vaidhyanathan, R.; Thangadurai, V.; Ratcliffe, C. I.; Moudrakovski, I. L.; Shimizu, G. K. H. *Nat. Chem.* **2009** *2009*, 9.